

# Evolution of volatile flavor compounds during roasting of nut seeds by thermogravimetry coupled to fast cycling optical heating gas chromatography-mass spectrometry with electron- and photoionization

Michael Fischer<sup>†‡</sup>, Sebastian Wohlfahrt<sup>†‡</sup>, Janos Varga<sup>†±</sup>, Georg Matuschek<sup>†</sup>, Mohammad R. Saraji-Bozorgzad<sup>†</sup>, Andreas Walte<sup>±</sup>, Thomas Denner<sup>#</sup>, Ralf Zimmermann<sup>†‡✉</sup>

<sup>†</sup>Joint Mass Spectrometry Centre, Institute of Chemistry, Chair of Analytical Chemistry, University of Rostock, 18057 Rostock, Germany

<sup>‡</sup>Joint Mass Spectrometry Centre, Cooperation Group “Comprehensive Molecular Analytics”, Helmholtz Zentrum München, 85764 Neuherberg, Germany

<sup>±</sup>University of Augsburg, Chair of Resource Strategy, 86159 Augsburg, Germany

<sup>†</sup>Research Unit Medical Radiation Physics and Diagnostics, Helmholtz Zentrum München, 85764 Neuherberg, Germany

<sup>†</sup>Photonion GmbH, 85764 Neuherberg, Germany

<sup>±</sup>Airsense Analytics GmbH, 19061 Schwerin, Germany

<sup>#</sup>Netzsch-Geraetebau GmbH, 95100 Selb, Germany

✉Corresponding author. Email: ralf.zimmermann@uni-rostock.de. Tel.: +49 (0) 89 3187 4544. Fax: +49 (0) 89 3187 3371.

## Abstract

Online multidimensional evolved gases analysis was conducted during the roasting of nuts using fast-cycling optical heating gas chromatography (OHGC) coupled to mass spectrometry with electron ionization and soft single photon ionization (OHGC-EI/SPI-MS). SPI is a semi-selective soft ionization method for organic

compounds that produces mainly molecular ions, whereas EI is a hard ionization method that results in fragmentation. Ionization was either exclusively by one of these methods, or both were used alternately. Roasting of the nuts (almonds, Brazil nuts, cashews, peanuts, hazelnuts, pecans, pine nuts, and walnuts) was simulated in a thermal analysis (TA) device at a roasting temperature of 170 °C. The TA device was directly coupled to the OHGC-EI/SPI-MS for quasi-real-time analysis. Multidimensional analysis was possible with a temporal resolution of 1 min. Good chromatographic separation, constant repetition rates, and constant retention times (RTs) were obtained. Peak assignment was performed using the molecular mass information obtained from SPI-MS, the characteristic fragmentation patterns from EI-MS, and the OHGC RTs. The gases that evolved during roasting of each type of nut were monitored online using the TA-OHGC-MS setup. Aldehydes, furans and pyrazines were detected as flavor compounds. Changes in the compositions of the evolved gases during the roasting process were evaluated. The TA-OHGC-MS method could separate isobaric and isomeric compounds.

### **Keywords**

Roasting; Nut; Flavor; Evolved gas analysis; Single photon ionization; Ultrafast gas chromatography

### **INTRODUCTION**

Thermal analysis (TA) is widely used in both research and industry to study the chemical and physical properties of materials. Modern TA systems combine thermogravimetry (TG) and differential scanning calorimetry. Detailed information on the chemical signature of a thermal process can be obtained by evolved gas analysis (EGA) (Raemakers and Bart 1997). EGA can be performed offline by sequential coupling of TA to gas chromatography mass spectrometry (Chiu 1968; He et al. 2015; Hof et al. 2014). Although coupling to chromatography provides high separation power, it sacrifices the temporal resolution of the thermal process. Coupling of TA with online methods, such as Fourier-transform infrared spectroscopy and mass spectrometry (TA-MS), allows for highly resolved real-time analysis of thermal reactions (Materazzi and Risoluti 2014; Materazzi and Vecchio 2013). TA-MS can be realized via capillary coupling or skimmed supersonic expansion (Celiz and Arii 2014; Kaisersberger and Post 1997; Kaisersberger and Post 1998; Saraji-Bozorgzad et al. 2011; Várhegyi et al. 2009). Standard TA-MS approaches using electron ionization (EI) cannot be used for samples with very complex matrices as the selectivity is low. To overcome this problem, some studies have reported the use of soft and selective ionization methods for natural samples (Fischer et al. 2013; Fischer et al. 2014). Recently, an additional fast gas chromatography (GC) separation step has been used between the TA and MS

with modulation of the evolved gases for quasi online TA-GC-MS (Saraji-Bozorgzad et al. 2010; Wohlfahrt et al. 2013).

The most common ionization technique for gases and vapors is EI, which is usually performed with an electron energy of 70 eV. EI has high ionization efficiency but causes high fragmentation of molecules. The fragments produced are characteristic for specific classes of molecules or functional groups, and identification of compounds is commonly conducted by comparison of data with spectral databases (e.g., NIST). However, fragmentation of co-existing compounds results in complex mass spectra that are difficult to interpret. This is common for complex matrices such as petroleum or other natural samples. In these cases, identification of individual compounds in online EGA without molecular ion information is often not possible. Consequently, soft ionization techniques such as chemical ionization, atmospheric pressure chemical ionization, and photo ionization (PI) have become preferred methods for direct fast detection of organic gaseous compounds (Cao et al. 2003; Hanley and Zimmermann 2009; Lindinger et al. 1993; Rüger et al. 2015). Single photon ionization (SPI) is performed at a lower energy (8–12 eV) than EI, and this has a number of advantages. First, because of the energetic threshold of vacuum ultraviolet (VUV) photons, only molecules with ionization potentials (IP) lower than the photon energy are ionized. Carrier gases like nitrogen (IP = 15.58 eV) and bulk gases like oxygen (IP = 12.06 eV), carbon dioxide (IP = 13.77 eV), and water (IP = 12.62 eV) are not ionized (Streibel et al. 2007). Second, soft ionization causes less fragmentation of the compounds and produces molecular ions. A number of studies have used PI for MS of complex organic matrices (Diab et al. 2014; Fischer et al. 2013; Hölzer et al. 2014; Isaacman et al. 2012; Jia et al. 2015; Schmid et al. 2013; Wu et al. 2010; Yang et al. 2009; Zimmermann et al. 2015).

The gases that evolve from natural products contain an enormous variety of compounds, including isobaric and isomeric compounds. To distinguish isobaric compounds, enhanced mass resolution of the MS might be sufficient. By contrast, for isomers, other methods such as chromatographic separation are necessary. Saraji et al. (2010) performed quasi real-time, online, multidimensional analysis by TA-GC-MS. Similarly to comprehensive two-dimensional gas chromatography, they used a cryogenic modulator to dissect a continuous stream of evolved gas into discrete samples, which were injected into a short GC column for isothermal fast-GC separation. This resulted in an additional separation dimension, and the cryogenic focusing effect decreased the limit of detection. If fast chromatographic separation is used in online analysis, EI could be applied without co-elution fragmentation problems because interferences will be reduced. Eschner et al. (2011) reported using EI and SPI in an alternating (or switching) mode, with the SPI producing molecular ions and EI producing

characteristic fragmentation patterns. Switching between the ionization methods enabled comprehensive peak assignment because the EI fragmentation patterns could be compared with spectral databases and the molecular ion information from SPI could be used to identify any co-eluted compounds or compounds not obvious in the spectral databases. There were some problems with Saraji's setup, including retention time (RT) shifting, but these problems could be overcome using an ultrafast-cycling optical heated GC (OHGC) (Fischer et al. 2015). Coupling of OHGC to TA-MS (TA-OHGC-MS) is beneficial because it provides improved chromatographic separation of isomeric and isobaric compounds with constant RTs, allows for easy peak assignment with the alternating EI/SPI-mode, and has a low limit of detection because of accumulation of compounds during modulation (cryofocusing effect).

Nuts are consumed worldwide both raw and after undergoing processing such as roasting. Many volatile compounds, which lead to unique flavors, are formed during roasting. Some flavor compounds, including aldehydes, furans, and pyrazines, are formed by Maillard and Strecker reactions, which lead to thermal degradation of sugars and lipid oxidation (Mottram 2007; Neta et al. 2010). Nut flavor is usually characterized after extraction of the volatile phase by steam distillation, high vacuum distillation, solvent extraction, simultaneous distillation–extraction, solvent-assisted flavor evaporation, or solid-phase micro extraction. Analysis of the volatile phase is generally performed by GC or GC-olfactometry (Krist et al. 2004; Neta et al. 2010; Schirack et al. 2006). Roasting of coffee beans has been investigated by online mass spectrometry (Dorfner et al. 2004; Gloess et al. 2014; Yeretizian et al. 2003), and roasting experiments with single beans have been performed with a microprobe sampling setup for PI mass spectrometry (Hertz-Schunemann et al. 2013b) and in a TA device (Fischer et al. 2014).

The aim of the current study was to apply TA-OHGC-MS to monitoring and online analysis of the evolved gases from nut roasting. The alternating (EI/SPI) ionization technique was used to support the assignment of  $m/z$  signals and aid identification of co-eluted compounds. The results can be used for characterization of various nuts according to their evolved gas composition.

## **MATERIALS AND METHODS**

Experiments were carried out using a modification of an established setup (Eschner et al. 2011; Saraji-Bozorgzad et al. 2010; Wohlfahrt et al. 2013), which is discussed below and shown in Fig. 1. Evolved gases from the TA-cell were continuously modulated in a cryogenic modulator, chromatographically separated on a GC column, ionized in the ion-source, and detected by a time-of-flight MS.

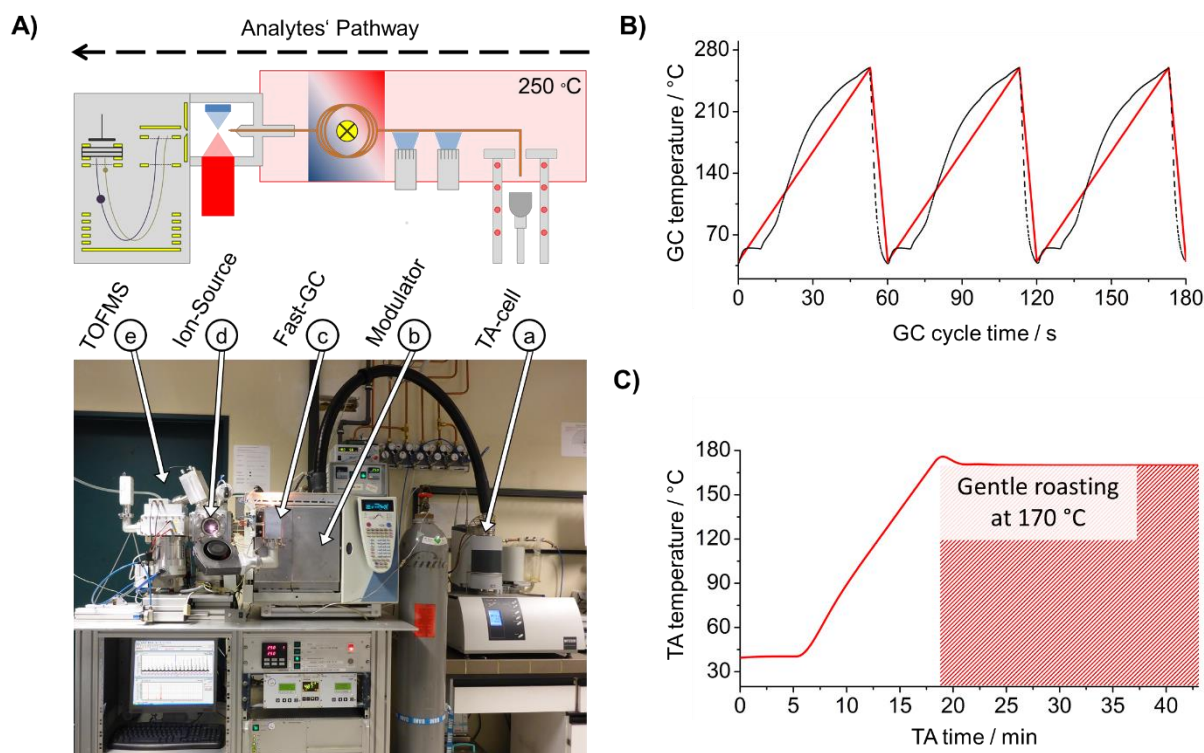


**Fig. 1 Experimental setup:** A) Schematic representation (top) and photograph of the TA-OHGC-MS setup, which include a TA-cell (a), cryogenic modulator (b), OHGC (c), ion-source (d), and time-of-flight MS (e). B) Theoretical (red line) and experimental (black line) heating (40 °C to 260 °C) and cooling cycles (60 s) of the fast-OHGC. C) The roasting program in the TA-cell.

### TA and Evolved Gases

A simultaneous TA device (STA 449 F3 Jupiter, Netzsch-Geraetebau GmbH, Selb, Germany) was connected to a two-dimensional gas chromatograph (Trace, Thermo Fisher Scientific, Waltham, MA) via a heated (250 °C) deactivated fused silica capillary (3 m × 180 µm i.d.), which was used as an interstage oven. Gases that evolved in the TA, which was at ambient pressure, were transported by a pressure gradient through the interstage oven into the ion source of the MS. To avoid cold spots and condensation of the evolved gases, the coupling points were heated to 250 °C.

### Cryogenic Modulator

Modulation of the evolved gases was conducted in cycles of 60 s using a cryogenic dual-jet CO<sub>2</sub> modulator in the interstage oven. In the CO<sub>2</sub> stream, the effluent was trapped on a column (BPX35, 0.2 m × 250 µm, 0.25 µm film thickness, SGE Analytical Science, Melbourne, Australia) and remobilized by the interstage oven heated to 250 °C.

## Ultrafast-cycling Gas Chromatography Module

The fast-OHGC module developed by Fischer et al. (2015) was added to the door side of the GC oven. The column was a BPX35 (3 m × 250 μm, 0.25 μm film thickness, SGE Analytical Science). The modulation time was set to 60 s and the temperature program involved heating from 40 °C to 260 °C. Figure 1B shows theoretical temperature curves and the experimental temperature curves, which were constructed using data from an integrated temperature sensor (0.25 mm, type K) acquired at a rate of 50 Hz. The number of theoretical plates ( $N$ ) and the height equivalent to the theoretical plates ( $H$ ) were calculated using a test gas of benzene, toluene, and xylene and the half-height method. The calculated  $N$  were 9451, 23652, and 56994 for benzene, toluene, and xylene, respectively, and the corresponding  $H$  were 0.32, 0.13, and 0.05 mm. A resolution ( $R$ ) of 1.97 was obtained for the isomers (*E,Z*)-2,4-decadienal and (*E,E*)-2,4-decadienal in a Brazil nut.

## Mass Analyzer and Ionization Method

Fast data acquisition was performed using a modified compact time-of-flight MS (TOFMS; CTOF, Tofwerk AG, Thun, Switzerland). The pressure in the ion source was dependent on the temperature in the fast-OHGC, and alternated between 3.3 and 4.8  $10^{-5}$  mbar. The pressure in the TOFMS was 3.3  $10^{-6}$  mbar. Ionization was by hard EI with an electron energy of 70 eV, and soft SPI with a photon energy of about 10.2 eV (at the Lyman-alpha line, 121.6 nm). Both ionization methods could be performed in an alternating mode (EI/SPI-mode), as detailed by Eschner et al. (Eschner et al. 2011). In the alternating mode, a quadrupole-mass-filter, which was placed in the ion source in front of the TOFMS, was used to eliminate signals as low  $m/z$ , including the carrier gas  $N_2$ . The switching frequencies at acquisition rates of 10 and 100 Hz were 5 and 50 Hz, respectively. For SPI, a water-cooled deuterium lamp (L 1835, Hamamatsu Photonics Deutschland GmbH, Herrsching, Germany) was used as the VUV source. The light beam was focused in the ionization chamber using a double parabolic mirror module equipped with 6 and 8 inch  $MgF_2$ -coated parabolic mirrors. VUV light sources are susceptible to loss of intensity in the VUV region over time, and the  $MgF_2$ -coating of the mirror was used to minimize this (Wilbrandt et al. 2012). The measurements were carried out with a deuterium lamp with a running time of 120–170 h.

## TA settings for nut roasting

For the roasting experiments, a single nut sample (approximately 1 g) was placed in a large  $Al_2O_3$  beaker in the TA cell (Figure S-1). To reach a sample mass of 1 g, a single whole seed (peanut, almond), more than one seed (e.g., three pine nuts) or seed pieces (brazil nut, cashew, hazelnut, pecan, walnut) were placed in the beaker. The samples were not pre-treated before analysis. After closing the furnace, the protective and purge gas flows were

set to 20 and 55 mL/min, respectively. To ensure that all ambient air (O<sub>2</sub>) was removed from the system to protect the capillary column of the OHGC, heating was not started until 5 min after the gas flows were initiated. Then, the TA was conducted isothermally for 5 min at 40 °C to stabilize the temperature in the fast-OHGC module and the CO<sub>2</sub> modulator. For post-processing of the data, this 5 min was subtracted from the data set as no mass loss occurred during this time. The sample was then heated to 170 °C with a heating rate of 10 C/min and held at 170 °C for 25 min (Figure 1C). After 25 min, the sample was removed from the TA cell to protect the system from the gases that were evolving from the roasted sample. Finally, the furnace was heated to 500 °C to clean the system and avoid carryover. During this cleaning step, the fast-OHGC module was operated. Similar to the method of Smith et al. (2014), the roasting temperature was set to 170 °C, but the roasting duration was increased from 15 min to 25 min so that it could be applied to all nut types in this study.

For comparison purposes, the data for all nut samples were normalized to a sample weight of 1 g in post-processing. Data processing and graphing were performed using Tofware and TofDaqViewer (Tofwerk AG, Thun, Switzerland), Microsoft Excel and Powerpoint (Microsoft Corporation, Redmond, USA), Matlab (The MathWorks Inc., Natick, USA), MarvinSketch (ChemAxon, Budapest, Hungary), and OriginPro (OriginLab Corporation, Northampton, USA).

## **Samples**

The following raw nuts were obtained for use in this study: almonds (*Prunus dulcis*), Brazil nuts (*Bertholletia excelsa*), cashews (*Anacardium occidentale*), peanuts (*Arachis hypogaea*), hazelnuts (*Corylus avellana*), pecans (*Carya illinoensis*), pine nuts (*Pinus pinea*), and walnuts (*Juglans regia*). All nuts were untreated and commercially available. Although peanuts are actually legumes, we refer to them as nuts in this study for simplicity.

## **RESULTS AND DISCUSSION**

During the simulated roasting process at 170 °C, a major mass loss occurred in the TG analysis, and this was attributed to water. This mass loss was influenced by the size, surface area, and water content of the nuts. Consequently, different types of nuts showed different TG profiles for the water loss. However, because the contents of volatile and flavor components were low compared with the water content, the TG results did not show characteristic signals for the different types of nuts (Figure S-2) and could not be used to evaluate the roasting process. Consequently, the TG data are not discussed further in this work. As an example, results for four replicates of the TG analysis of peanut roasting are shown in Figure S-3.

Instead of using TG data, an initial evaluation of the roasting process for the different nuts was conducted using time-resolved EI and SPI MS three-dimensional plots (Fig. 2). In earlier studies, such as monitoring of gases produced during roasting in laboratory experiments (Dorfner et al. 2004) or in industrial roasters (Hertz-Schunemann et al. 2013a), these types of plots have been used.

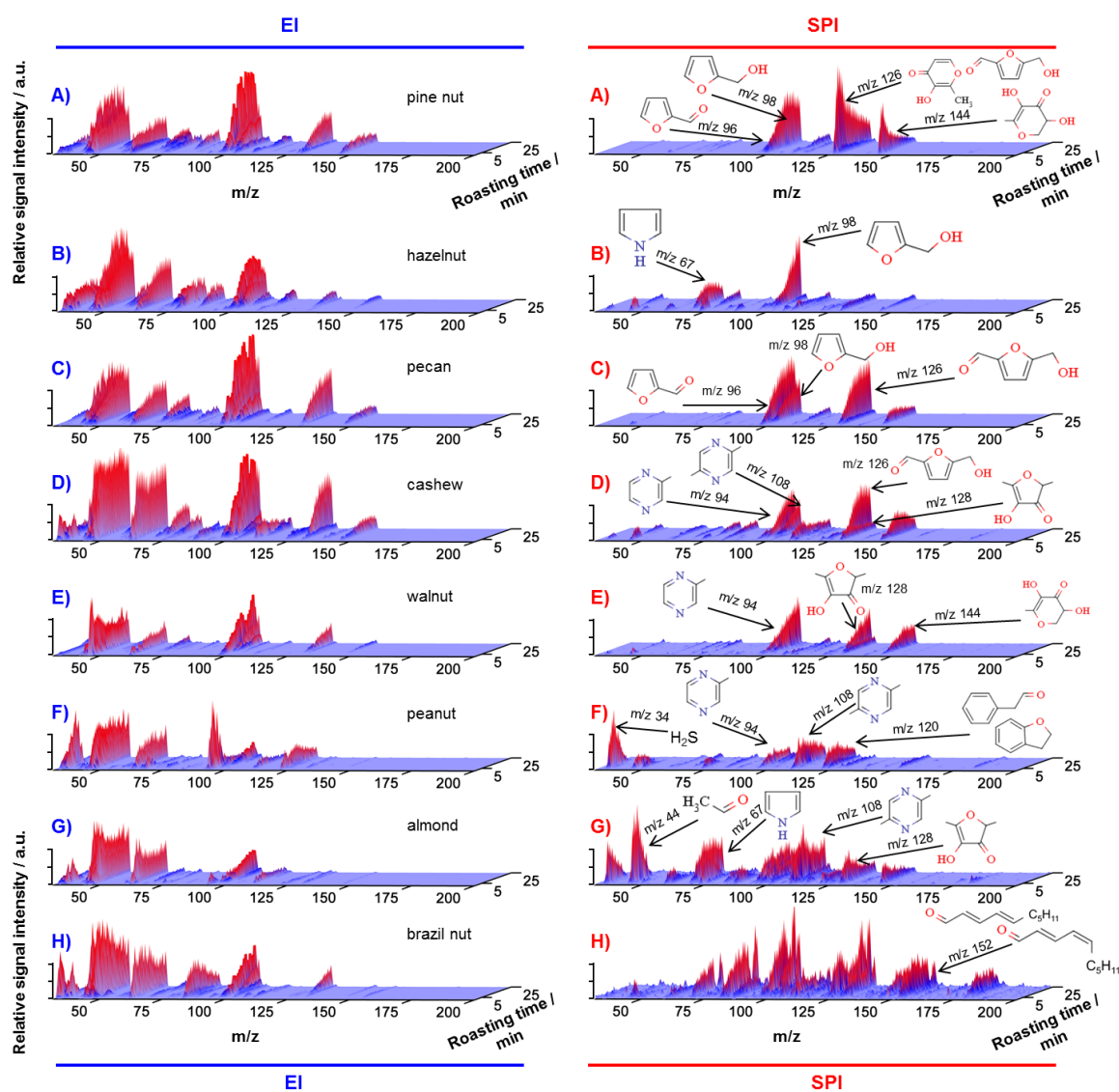


**Fig. 2** Three-dimensional plots of the results obtained by TA-MS with hard (EI, left column) and soft (SPI, right column) ionization for A) pine nuts, B) hazelnuts, C) pecans, D) cashews, E) walnuts, F) peanuts, G) almonds, and H) Brazil nuts during 25 min of gentle roasting.

Although GC separation was performed in this study, the GC results are not displayed in these plots. Therefore, these plots are representative of the results that would be obtained using TG-MS without GC separation. The plots clearly show the differences between the two ionization methods. Whereas SPI (right column) mainly produces molecular ions with large molecular masses, EI predominately generates fragments with small



molecular masses. Therefore, EGA using SPI will be more powerful than that using EI because molecular masses will be rather interpretable than overlaying fragments from EI. The EI-MS plots (left column) showed some fragment signals in the low  $m/z$  region that were present for all types of nuts, and some signals for what were assumed to be molecular ions. By comparison, the signals for the eight types of nuts (Fig. 2A–H) obtained using SPI-MS were more characteristic as the molecular masses and the signal intensities of the evolved gases varied considerably among the different nuts. The general trend was a decrease in the signal intensities from the pine nuts (Fig. 2A) to the Brazil nuts (Fig. 2H). Many of the components detected in the almonds (Fig. 2G) and Brazil nuts (Fig. 2H) were also present in the other nuts, but their signals were difficult to detect because their intensities were very low compared with those of other components. Consequently, for better visualization, the intensities in the plots were converted to relative signal intensities by normalizing to the highest signal for each nut.

The signals obtained by TA-OHGC-MS with alternating ionization methods were assigned according to molecular ions (SPI) and fragmentation patterns (EI). For the TA-SPI-MS results, the assignments for the signals were made with reference to literature data, and confirmed using the OHGC results. For the pine nuts (Fig. 2A) signals from SPI at  $m/z$  96 (furfural),  $m/z$  98 (2-furanmethanol),  $m/z$  126 (4H-pyran-4-one 5-hydroxymethylfurfural) and  $m/z$  144 (3,5-dihydroxy-6-methyl-2,3-dihydro-4H-pyran-4-one) were dominant. During the roasting process, the intensities of the signals at  $m/z$  126 and 144 increased rapidly at the beginning of the process, and then decreased after a few minutes. By contrast, the intensity of the signal for 2-furanmethanol ( $m/z$  98) increased from the beginning of the process until 15 min, and then stayed constant until the end of the process. The evolved gases from the hazelnuts (Fig. 2B) showed many signals, with the signal at  $m/z$  98 being dominant. The changes in the signal intensity for 2-furanmethanol during roasting of hazelnuts and pine nuts were similar, but the signal intensity started increasing at a later point in the process for pine nuts compared with hazelnuts. In addition, the signal intensity increased throughout the process for hazelnuts but stayed constant after a certain point for pine nuts. Pecans (Fig. 2C) showed high signal intensities for furfural, which was the dominant component, 2-furanmethanol, and 4H-pyran-4-one, 5-hydroxymethylfurfural. These signal intensities were also high for the cashews (Fig. 2D). Other high intensity signals for the cashews included  $m/z$  108 (2,5-dimethylpyrazine),  $m/z$  128 (2,5-dimethyl-4-hydroxy-3(2H)-furanone) and  $m/z$  144 (3,5-dihydroxy-6-methyl-2,3-dihydro-4H-pyran-4-one). The roasting profile for the walnuts (Fig. 2E) was very similar to that for the pecans (Fig. 2C), which is not surprising because they belong to the same botanical family (*Juglandaceae*). The composition of the evolved gas from the peanuts (Fig. 2F) was different from the other nuts. Initially, signals at

$m/z$  34 (hydrogen sulfide),  $m/z$  44 (acetaldehyde), and  $m/z$  74 (1-hydroxy-2-propanone) were observed. The higher mass region was dominated by  $m/z$  94 (methylpyrazine),  $m/z$  108 (2,5-dimethylpyrazine), and  $m/z$  120 (benzeneacetaldehyde and 2,3-dihydrobenzofuran, double peak as shown in Fig. 3), which was not observed for the other nuts. For the almonds (Fig. 2G), there were few dominant signals and many low intensity signals. The most abundant signals were at  $m/z$  34 (hydrogen sulfide), 44 (acetaldehyde), 67 (pyrrole), 72 (2-methylpropanal), 94 (methylpyrazine), 96 (furfural), 98 (2-furanmethanol), 108 (2,5-dimethylpyrazine) and 128 (2,5-dimethyl-4-hydroxy-3(2H)-furanone). Prominent signals in the roasting profile of the Brazil nuts were at  $m/z$  67 (pyrrole), 96 (furfural), 98 (2-furanmethanol), 126, (4H-pyran-4-one) and 152 ((*E,Z*)-2,4-decadienal and (*E,E*)-2,4-decadienal). These results show that the three-dimensional plots present an overview of the roasting processing and can be used to establish fingerprint mass spectra according to the components detected in the evolved gases for the nuts.

Fig. 3 shows the total ion current (TIC) chromatograms for peanuts and hazelnuts after roasting. The selected signals for selected ion monitoring mode (SIM) were  $m/z$  81 (peanuts, Fig. 3A), 86 (hazelnuts, Fig. 3B), and 120 (peanuts, Fig. 3C). These figures are used to show how chromatographic separation of isobaric compounds was achieved and the signals for these compounds were assigned. The samples were ionized with either EI (blue figures and marker on left hand side) or SPI (red figures and marker on left hand side). Initially, during temperature stabilization and heating, the signal intensities were low in all the TICs. After 18 min, when the roasting temperature of 170 °C was reached, the signal intensities started to increase. During roasting, individual modulation/fast-GC separation cycles were visible in the TICs, and were even more obvious in SIM. For each nut and ionization method, one modulation/fast GC-separation cycle (labeled as Cycle on the figure) of 60 s was magnified. For EI, this revealed several separate peaks at the selected  $m/z$ , which were characteristic of high fragmentation. For SPI, this showed a few separate peaks for SPI, which were characteristic of molecular ion production. The EI fragmentation patterns were compared with data in the NIST library for peak assignment.

When evaluating the signal at  $m/z$  81 for peanuts, co-elution hindered the assignment of the peaks. In this case, the alternating mode of ionization was useful because SPI provided molecular ion information that could be used for peak assignment. By comparison, EI did not provide any molecular ions as the dominant peaks were for fragments of 2,5-dimethylpyrazine and 2-pentylfuran. A signal appeared at  $m/z$  94 (methylpyrazine) in both the EI and SPI results (labeled MS2 on the figure), and information from SPI (labeled D on the figure) indicated that this signal was actually for co-eluted compounds (3-methyl-1H-pyrrole and methylpyrazine). This information enabled signal assignment for the EI fragmentation pattern. Finally, comparison of NIST data

(labeled NIST 1 and NIST 2 on the figure) with peaks 1 and 2 (labeled as MS1 and MS2 on the figure) was used to assign these as 1-methyl-1H-pyrrole and 3-methyl-1H-pyrrole, respectively.

For the signal at  $m/z$  86 from hazelnut roasting (Fig. 3B), peaks 3 and 4 were present in both the EI and SPI results. In the EI results, different fragmentation behavior was observed for these components. Peak 3, which was assigned to 2,3-butanedione (ketone), had a high signal intensity for the fragment at  $m/z$  43 and a low intensity for the molecular ion peak  $m/z$  86 (labeled as MS 3 on the figure). By contrast, peak 4, which was assigned to 2-methylbutanal (aldehyde), was highly fragmented with dominant signals at  $m/z$  41, 57, 58 and a low intensity signal at  $m/z$  86 (MS 4).

For the signal at  $m/z$  120 from peanut roasting (Fig. 3C), peak 5 and 6 were observed in both the EI and SPI results and were well separated and intense. The components of peak 5 and peak 6 showed different fragmentation patterns in the EI-MS (labeled as MS 5 and MS 6 on the figure). Comparison with spectra from the NIST database (labeled as NIST 5 and NIST 6 on the figure) was used to assign peak 5 as benzeneacetaldehyde and peak 6 as 2,3-dihydrobenzofuran.

Using the process described above, the molecular ion information from SPI, EI fragmentation patterns, and characteristic RTs were used to assign peaks for all the nuts tested in this study (Table 1). All  $m/z$  values listed in Table 1 were selected using only SPI, and then assigned using the alternating mode. Further details from the EI and SPI mass spectra and the corresponding NIST EI mass spectra are given in Table S-1.

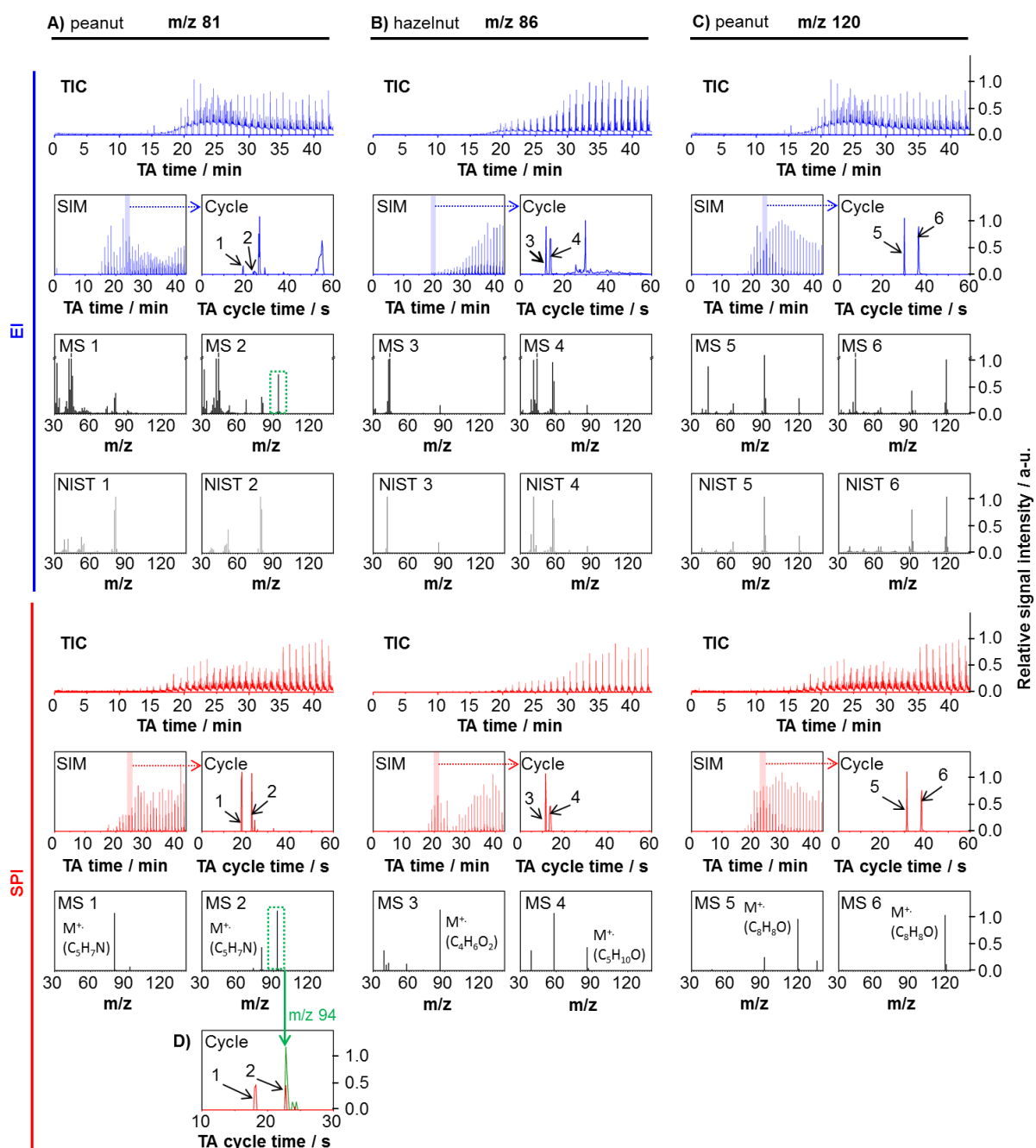


**Fig. 3** Separation of isobaric compounds by fast-cycling optical heating gas chromatography for selected signals from peanuts (A =  $m/z$  81 and C =  $m/z$  120) and hazelnuts (B =  $m/z$  86) after roasting. The figures are for EI (blue) and SPI (red) and show total ion current (TIC) chromatograms, selected ion monitoring (SIM) chromatograms for the entire TA process, SIM chromatograms for one OHGC 60 s cycle (Cycle) in the TA process, selection of two distinct peaks (MS 1 and MS 2; MS 3 and MS 4; MS 5 and MS 6) in these cycles and their fragmentation pattern from EI and molecular ions from SPI.

The RT is dependent on the OHGC program, the type of column used for separation, and the column length. If these parameters are stable, the RT can be used in combination with the molecular ions for peak assignment of compounds in the evolved gases from roasting of the nuts. However, there are exceptions concerning constant

RTs. This behavior will be explained in the following. Although water was not detected directly using either SPI or EI because of the ionization threshold (SPI) and the activated mass filter (EI), it is a major component in the roasting gases and causes RT shifts, especially for highly polar components such as acetic acid and 1-hydroxy-2-propanone. Interaction of these components with the stationary phase of the GC column is affected by the presence of water, and their RTs decrease from cycle to cycle. This behavior was reproducible within various experiments. In addition, for components with longer RTs, some overlapping may occur because of insufficient chromatographic separation. In these cases, assignment according to EI fragmentation patterns is not possible with the described approach.

**Table 1** List of compounds in the evolved gases from the roasting of various nuts.

Nr.	Almond	Brazil nut	Cashew	Hazelnut	Peanut	Pecan	Pine nut	Walnut	RT <sup>b</sup> [s]	m/z	Compound
1	•		•	•	•				8.8 ±0.13	34	Hydrogen sulfide
2	•		•	•	•	•		•	9.1 ±0.10	44	Acetaldehyde (Mason et al. 1967; Walradt et al. 1971)
3	•		•	•	•				9.8 ±0.10	58	Propanal (Acetone)(Smith and Barringer 2014; Su et al. 2011; Walradt et al. 1971)
4	•	•	•	•	•	•	•	•	<sup>a</sup>	60	Acetic acid
5	•	•	•	•	•	•	•	•	19.8 ±0.24	67	Pyrrole
6	•		•	•	•				10.8 ±0.21	72	2-Methylpropanal
7	•		•	•		•	•	•	<sup>a</sup>	74	1-Hydroxy-2-propanone
8		•	•	•	•				18.8 ±0.16	81	1-Methyl-1H-pyrrole
9	•	•	•	•	•	•			23.6 ±0.25	81	3-Methyl-1H-pyrrole
10	•			•	•		•		11.7 ±0.19	86	2,3-Butanedione
11	•			•	•				13.6 ±0.30	86	2-Methylbutanal
12	•	•	•	•	•	•	•	•	23.5 ±0.16	94	Methylpyrazine
13			•			•	•		31.5 ±0.24	95	2-Carboxaldehyde-1H-pyrrole-
14	•	•	•	•	•	•	•	•	24.2 ±0.19	96	Furfural
15			•			•		•	26.6 ±0.11	96	4-Cyclopentene-1,3-dione
16	•	•	•	•	•	•	•	•	24.4 ±0.24	98	2-Furanmethanol

17	•	•		•	22.7 ±0.15	100	Dihydro-2-methyl-3(2H)-furanone		
18	•			•	27.2 ±0.01	104	Methional		
19	•	•	•	•	•	•	26.3 ±0.17	108	2,5-Dimethylpyrazine
20	•		•	•	•	•	28.6 ±0.17	110	5-Methyl-2-furancarboxaldehyde
21		•		•	•	•	32.4 ±0.20	114	2-Furfurylthiol, 2-heptanone, heptanal(Chung et al. 1993; Diab et al. 2014; Neta et al. 2010)
22	•		•	•			31.0 ±0.93	120	Benzeneacetaldehyde
23				•			38.9	120	2,3-Dihydrobenzofuran
24	•		•	•		•	28.9 ±0.20	122	2-Ethyl-5-methylpyrazine
25			•	•	•	•	34.5 ±0.79	126	4H-Pyran-4-one
26	•	•	•	•		•	41.2 ±0.26	126	5-Hydroxymethylfurfural
27	•	•	•	•	•	•	32.1 ±0.19	128	2,5-Dimethyl-4-hydroxy-3(2H)-furanone
28		•		•			31.0 ±0.21	136	3-Ethyl-2,5-dimethylpyrazine
29		•	•		•	•	28.2 ±0.22	144	2,4-Dihydroxy-2,5-dimethyl-3(2H)-furan-3-one
30	•	•	•	•		•	35.8 ±0.25	144	2,3-Dihydro-3,5-dihydroxy-6-methyl-4H-pyran-4-one
31				•			41.8	150	2-Methoxy-4-vinylphenol
32	•						39.2	152	(E,Z)-2,4-Decadienal
33	•						40.4	152	(E,E)-2,4-Decadienal

<sup>a</sup>: The reaction time (RT) of the component was greatly influenced by the water content of the sample. Thus, a fixed RT was not defined in this study. The GC RTs were taken from the 8th or the 16th modulation cycle of roasting, depending on the analyte's occurrence.

<sup>b</sup>: The standard deviation was calculated using the number of nut samples that the component was present in (number of black dots in a row).

The RTs for the detected compounds of a peanut roasting experiment are shown in three-dimensional plots in Fig. 4. The three-dimensional plots were constructed with the RT on the *z*-axis, the roasting duration on the *y*-axis, and *m/z* on the *x*-axis for both EI (Fig. 4A) and SPI (Fig. 4B) results for peanuts. Signals with constant RTs appear as straight lines that are parallel to the roasting duration. These plots highlight areas where one ionization

method is better than the other. Lipid components in the high RT region (50–60 s) are ionized relatively efficiently by EI but this method results in high fragmentation. By contrast, SPI is relatively inefficient in this RT region, but results in less fragmentation. Because of the high EI fragmentation and inefficiency of SPI in this region, it was not possible to assign these signals.

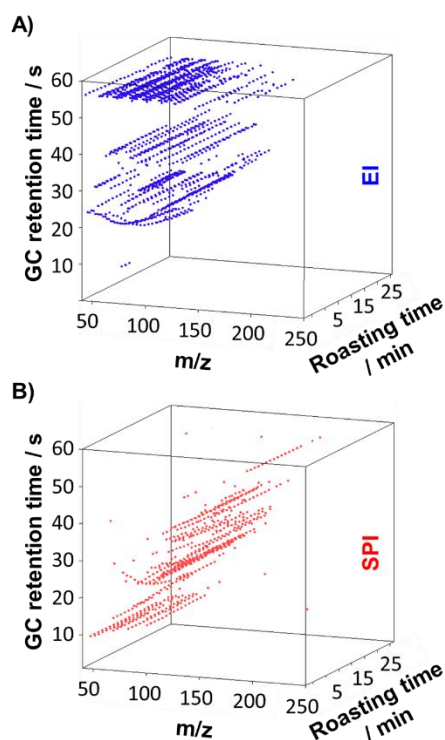


**Fig. 4** Three-dimensional TIC plots for analysis of a single peanut with EI (A) and SPI (B).

The peanut roasting results revealed that the signal at  $m/z$  120 was characteristic for this type of nut (Fig. 3). This could be attributed to the fact that peanuts are legumes not tree nuts like the other nuts used in this study. Changes in the signal at  $m/z$  120 were monitored during the roasting process for four individual peanuts (Fig. 5A a–d). The masses of the samples were different (a = 1180 mg, b = 1178 mg, c = 958 mg, d = 924 mg), and for comparison purposes, the ion signals were normalized to a mass of 1 g. The SIM chromatograms of the signal at  $m/z$  120 showed two independent peaks (Fig. 3), which were identified as benzeneacetaldehyde (dotted blue line) and 2,3-dihydrobenzofuran. The level of benzeneacetaldehyde, which has a flavor described as floral, sweet and green, increased initially during roasting and reached a maximum after 4–5 min. The level of benzeneacetaldehyde then decreased until after 12–15 min. The aroma of 2,3-dihydrobenzofuran is described as rubbery and harsh. During the roasting process, its level increased until it reached a maximum at 10–15 min, and then decreased slightly but was still present after 25 min of roasting (Neta et al. 2010; Schirack et al. 2006). The optimum roasting duration will depend on the mass of the nut. In previous experiments, it was determined that

roasting for 10–15 min at 170 °C gave an optimal grade of peanut roasting (optically rated). This roasting duration compares well with that in an earlier study (Smith and Barringer 2014). The benzeneacetaldehyde profiles (Fig. 5) combined with visual analysis of the roasting result indicate that the decrease in benzeneacetaldehyde could be used as an indicator of the optimum roasting duration for peanuts. Even though different peanuts will naturally have differences in composition, the signals at  $m/z$  120 for the four individual peanut roasting experiments were relatively constant (as shown by the error bars in Fig. 5B). This shows that this method is reproducible.

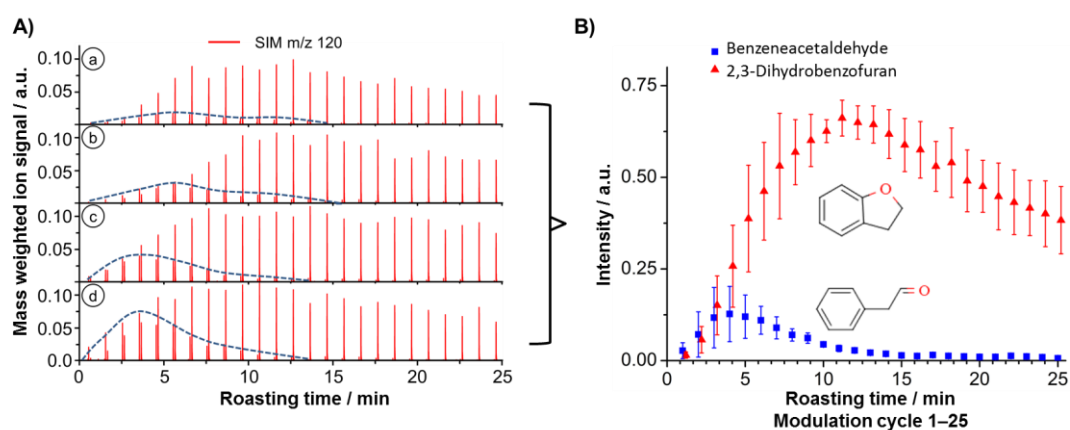


**Fig. 5** A) Changes in the signal at  $m/z$  120 during gentle roasting of four individual peanuts (a–d), showing two isobaric compounds with different temporal behavior. The blue dotted line highlights the peaks for benzeneacetaldehyde, while the remainder of the peaks are for 2,3-dihydrobenzofuran. B) Roasting profiles for  $m/z$  120 over 25 modulation cycles with the standard deviation ( $n = 4$ ).

## Flavor Compounds

We then investigated specific classes of flavor compounds that were detected in the evolved gases from the roasted nuts.

### Aldehydes

The signal at  $m/z$  152 could be attributed to two isomers of 2,4-decadienal, and we evaluated the EI (blue) and SPI (red) results obtained over 19 min of roasting of a Brazil nut to study these isomers (Fig. 6). Both (*E,Z*)-2,4-decadienal, which has a fatty, green odor, and (*E,E*)-2,4-decadienal, which has a fatty, deep fried odor, were released during the roasting process (Matsui et al. 1998). The EI and SPI signals showed the same trends for these compounds. The ion signal was weaker in SPI than EI, and these traces were noisier. Decadienal formation increased until 12 min, and then decreased until the end of the roasting process. Separation of the isomers was



evaluated using a magnification of the results for modulation cycle 12. Two major peaks were detected and were assigned to (*E,Z*)-2,4-decadienal (A) and (*E,E*)-2,4-decadienal (B). These two compounds were unique to the Brazil nut profile among the roasting experiments in this study, and could be considered as markers for Brazil nuts. These results show that TA-OHGC-MS can be used for separation of isomers.

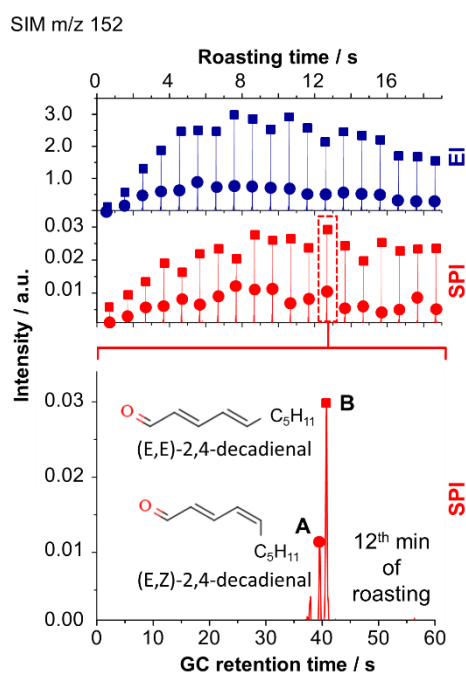


**Fig. 6** EI (blue) and SPI (red) SIM traces of the signal at  $m/z$  152 (circles = (*E,Z*)-2,4-decadienal, squares = (*E,E*)-2,4-decadienal) for Brazil nuts during gentle roasting, and a magnification of SIM trace in the 12<sup>th</sup> SPI modulation cycle (A = (*E,Z*)-2,4-decadienal, B = (*E,E*)-2,4-decadienal).

## Pyrazines

Pyrazines are considered key flavor compounds in roasted peanuts, with studies showing their concentrations are highly correlated with roasted flavor and aroma, especially for 2,5-dimethylpyrazine (Baker et al. 2003; Neta et al. 2010). To compare these earlier results with the present TA-OHGC-MS results, the modulation cycle after 15 min of peanut roasting was examined for pyrazines. Four pyrazines were detected, including 2-methylpyrazine ( $m/z$  94), 2,5-dimethylpyrazine ( $m/z$  108), 2-ethyl-5-methylpyrazine ( $m/z$  122) and 3-ethyl-2,5-dimethylpyrazine ( $m/z$  136) (Fig. 7). Similar to the results of Baker et al. (2003), 2,5-dimethylpyrazine ( $m/z$  108) was the most abundant pyrazine followed by 2-methylpyrazine ( $m/z$  94).

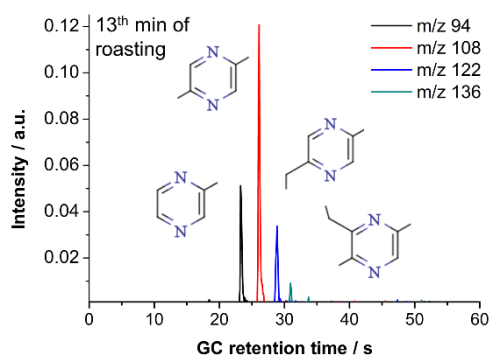


**Fig. 7** Pyrazines detected in the evolved gas from peanut roasting in the 16<sup>th</sup> modulation cycle (16 min of roasting) with SPI-MS. The peaks are assigned as follows: 2-methylpyrazine ( $m/z$  94), 2,5-dimethylpyrazine ( $m/z$  108), 2-ethyl-5-methylpyrazine ( $m/z$  122), and 3-ethyl-2,5-dimethylpyrazine ( $m/z$  136).

We then looked at the levels of these two pyrazines (2-methylpyrazine and 2,5-dimethylpyrazine) in all the types of nuts for the whole roasting duration with SPI-MS (Fig. 8). The most obvious finding was that the pecans and walnuts, which belong to the same family, showed the lowest signal intensities for the two pyrazines. When looking at the ratio of the signal intensity for  $m/z$  94 to that at  $m/z$  108, this ratio was very different for Brazil nuts compared with the other types of nuts. For Brazil nuts, 2-methylpyrazine was the dominant species. For the other types of nuts, both pyrazines were present with 2,5-dimethylpyrazine ( $m/z$  108) dominating for the first half of the roasting process and equal contribution from the two pyrazines for the remainder of the roasting process. Although the signal intensities varied, the trends and the ratios of  $m/z$  94 to  $m/z$  108 were relatively consistent for measurements within the same family (Fig. S-4).

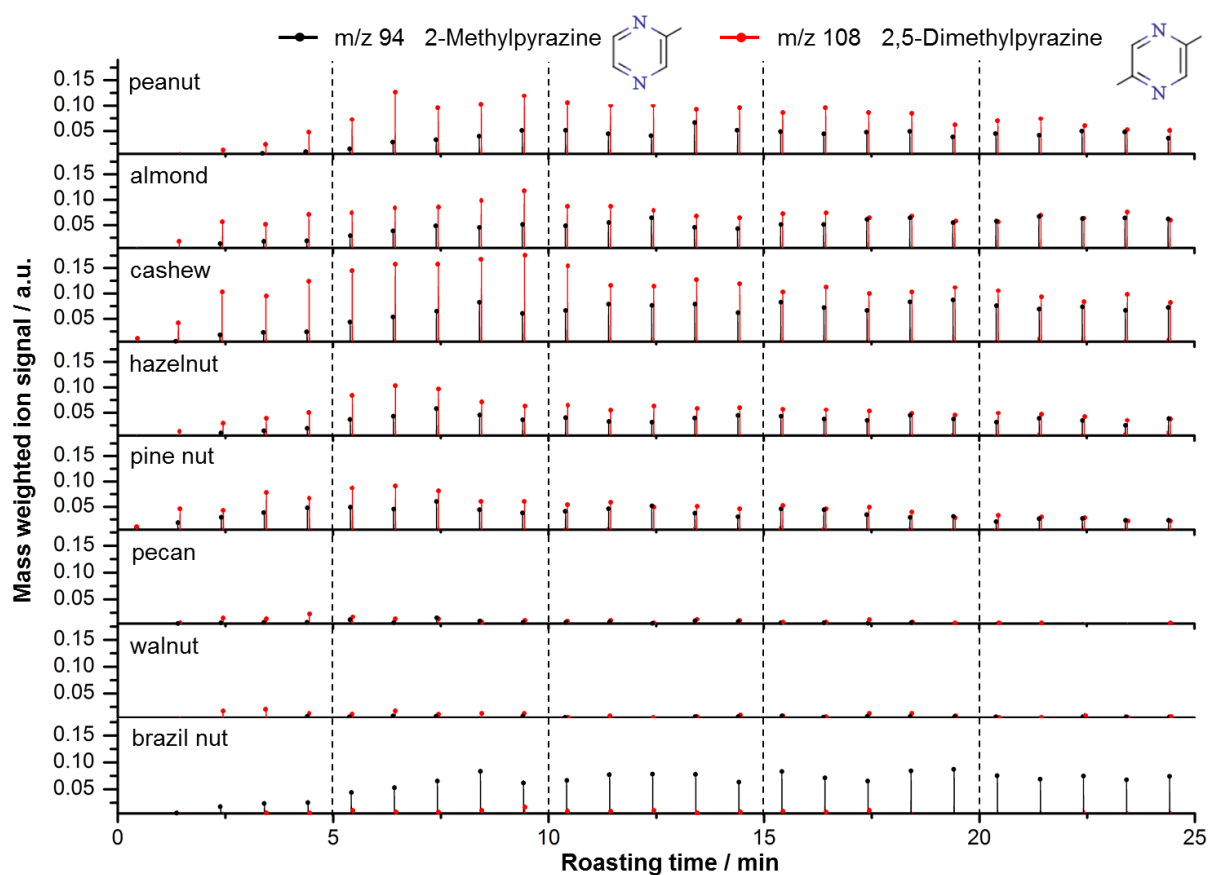


**Fig. 8** SIM traces showing the formation of key flavor compounds, 2-methylpyrazine ( $m/z$  94) and 2,5-dimethylpyrazine ( $m/z$  108), for various nuts during roasting at 170 °C.

### Furans and furan derivatives

Example results from the almonds, pine nuts, pecans, and walnuts for furans and furan derivatives are discussed in this section. After 15 min of roasting and during the 16<sup>th</sup> modulation cycle, five different compounds were detected for these nuts (Fig. 9). These compounds were furfural at  $m/z$  96 (1, black), 2-furanmethanol at  $m/z$  98 (2, red), 5-methyl-2-furancarboxaldehyde at  $m/z$  110 (3, blue), 5-hydroxymethylfurfural at  $m/z$  126 (4, green), and 2,5-dimethyl-4-hydroxy-3(2H)-furanone at  $m/z$  128 (5, pink). It should be noted that the signal at  $m/z$  126 observed for the pine nuts (dashed green line) was not a furan. The signal at  $m/z$  128 (2,5-dimethyl-4-hydroxy-3(2H)-furanone) was dominant in the almonds. All nuts showed high signal intensities for furfural ( $m/z$  96), 2-furanmethanol ( $m/z$  98), and 5-hydroxymethylfurfural ( $m/z$  126). These results show that the specific furans detected in the evolved gases from roasted nuts depends on the type of nut type, and the furan composition allows for a quick evaluation to distinguish between types of nuts.

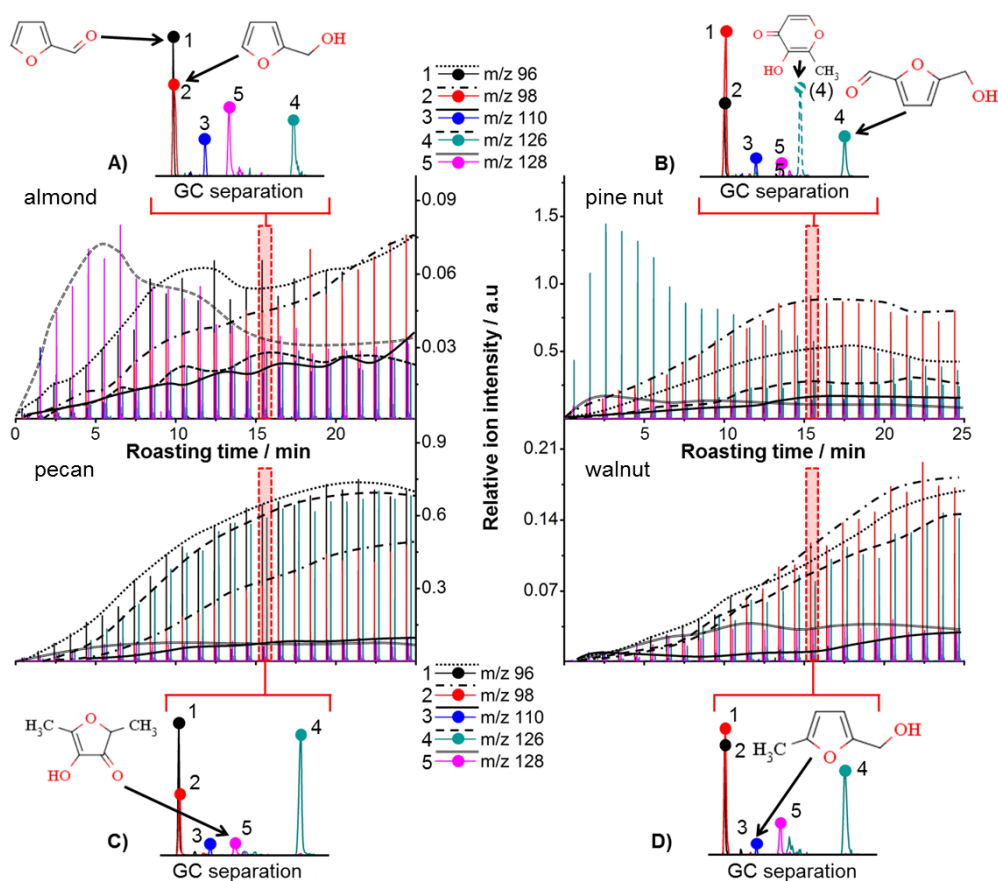


**Fig. 9** Furans and furan derivatives detected for almonds (A), pine nuts (B), pecans (C) and walnuts (D). Magnifications of the OHGC separation are shown after 15 min of roasting at 170 °C, with the detected compounds labeled as (1) furfural, (2) furfuryl alcohol, (3) 5-methyl-2-furancarboxaldehyde, (4) 5-hydroxymethylfurfural, and (6) 2,5-dimethyl-4-hydroxy-3(2H)-furanone.

## CONCLUSIONS

Multidimensional analysis of evolved gases from roasting of different types of nuts was carried out by TA coupled to modulated ultrafast-cycling OHGC using both SPI and EI. The OHGC separation gave high chromatographic resolution and constant RTs, and could be used for separation and identification of isobaric and isomeric compounds. Modulation steps resulted in concentration of the analytes and sharp chromatographic peaks enabled the detection of low compound concentrations in the roast gases. This enabled detection of compounds present at low concentrations in the roasting gases. Use of both SPI and EI combined the advantages of soft and hard ionization, and these methods could be used either exclusively or in an alternating mode. The characteristic RTs and results obtained with the different ionization methods allowed for rapid peak assignment for specific components in the roasting gases. The ideal roasting durations for peanuts could be determined by monitoring the composition of the roasting gas.

Modulation cycles of 60 s were sufficient for quasi-online analysis in nut roasting. Many of the components were separated on the GC column, but with the short column length, some components co-eluted and gave overlapping fragmentation patterns with EI. The molecular ions produced by soft ionization technique with SPI were used to overcome this problem with co-elution.

In conclusion, TA-OHGC-MS is a powerful analytical technique for applied and fundamental research in the food sciences and food industry. It provides a simple and rapid technique for real-time monitoring of key flavor compounds, such as pyrazines and furans, in thermal processing of food (e.g., roasting, toasting, baking). In addition to the investigation of thermal processing of food, it could be applied to tests with model substances to investigate individual flavor formation reactions (e.g., the Maillard reaction) and processes.

### **Acknowledgments**

Funding from the Bavarian Research Foundation (Bayerische Forschungsförderung, Az. 913/10) and support from Netzsch-Geraetebau and Photonion is gratefully acknowledged.

### **Compliance with Ethical Standards**

Funding: This study was funded by the Bavarian Research Foundation (Grant No. 913/10).

Conflict of Interest: Michael Fischer declares that he has no conflict of interest.  
Sebastian Wohlfahrt declares that he has no conflict of interest.  
Janos Varga declares that he has no conflict of interest.  
Georg Matuschek declares that he has no conflict of interest.  
Mohammad R. Saraji-Bozorgzad declares that he has no conflict of interest.  
Andreas Walte declares that he has no conflict of interest.  
Thomas Denner declares that he has no conflict of interest.  
Ralf Zimmermann declares that he has no conflict of interest.

Ethical approval: This article does not contain any studies with human participants or animals performed by any of the authors.

Informed consent: Not applicable.

## References

- Baker GL, Cornell JA, Gorbet DW, O'Keefe SF, Sims CA, Talcott ST (2003) Determination of Pyrazine and Flavor Variations in Peanut Genotypes During Roasting *Journal of Food Science* 68:394-400 doi:10.1111/j.1365-2621.2003.tb14171.x
- Cao L, Muhlberger F, Adam T, Streibel T, Wang HZ, Kettrup A, Zimmermann R (2003) Resonance-enhanced multiphoton ionization and VUV-single photon ionization as soft and selective laser ionization methods for on-line time-of-flight mass spectrometry: Investigation of the pyrolysis of typical organic contaminants in the steel recycling process *Analytical Chemistry* 75:5639-5645 doi:10.1021/ac0349025
- Celiz L, Ariei T (2014) Study on thermal decomposition of polymers by simultaneous measurement of TG–DTA and miniature ion trap mass spectrometry equipped with skimmer-type interface *J Therm Anal Calorim* 116:1435-1444 doi:10.1007/s10973-014-3817-0
- Chiu J (1968) Polymer characterization by coupled thermogravimetry-gas chromatography *Analytical Chemistry* 40:1516-1520 doi:10.1021/ac60266a037
- Chung TY, Eiserich JP, Shibamoto T (1993) Volatile compounds identified in headspace samples of peanut oil heated under temperatures ranging from 50 to 200.degree.C *Journal of Agricultural and Food Chemistry* 41:1467-1470 doi:10.1021/jf00033a022
- Diab J, Hertz-Schünemann R, Streibel T, Zimmermann R (2014) Online measurement of volatile organic compounds released during roasting of cocoa beans *Food Research International* 63, Part C:344-352 doi:10.1016/j.foodres.2014.04.047
- Dorfner R, Ferge T, Yeretian C, Kettrup A, Zimmermann R (2004) Laser Mass Spectrometry as On-Line Sensor for Industrial Process Analysis: Process Control of Coffee Roasting *Analytical Chemistry* 76:1386-1402 doi:10.1021/ac034758n
- Eschner MS, Gröger TM, Horvath T, Gonin M, Zimmermann R (2011) Quasi-Simultaneous Acquisition of Hard Electron Ionization and Soft Single-Photon Ionization Mass Spectra during GC/MS Analysis by Rapid Switching between Both Ionization Methods: Analytical Concept, Setup, and Application on Diesel Fuel *Analytical Chemistry* 83:3865-3872 doi:10.1021/ac200356t
- Fischer M et al. (2013) Thermal analysis/evolved gas analysis using single photon ionization *J Therm Anal Calorim* 113:1667-1673 doi:DOI 10.1007/s10973-013-3143-y
- Fischer M et al. (2015) Optically Heated Ultra-Fast-Cycling Gas Chromatography Module for Separation of Direct Sampling and Online Monitoring Applications *Analytical Chemistry* 87:8634-8639 doi:10.1021/acs.analchem.5b01879
- Fischer M, Wohlfahrt S, Varga J, Saraji-Bozorgzad M, Matuschek G, Denner T, Zimmermann R (2014) Evolved gas analysis by single photon ionization-mass spectrometry *J Therm Anal Calorim*:1-9 doi:10.1007/s10973-014-3830-3
- Gloess AN et al. (2014) Evidence of different flavour formation dynamics by roasting coffee from different origins: On-line analysis with PTR-ToF-MS *International Journal of Mass Spectrometry* 365–366:324-337 doi:10.1016/j.ijms.2014.02.010
- Hanley L, Zimmermann R (2009) Light and Molecular Ions: The Emergence of Vacuum UV Single-Photon Ionization in MS *Analytical Chemistry* 81:4174-4182 doi:10.1021/ac8013675
- He Q, Wan K, Hoadley A, Yeasmin H, Miao Z (2015) TG–GC–MS study of volatile products from Shengli lignite pyrolysis *Fuel* 156:121-128 doi:10.1016/j.fuel.2015.04.043
- Hertz-Schunemann R, Dorfner R, Yeretian C, Streibel T, Zimmermann R (2013a) On-line process monitoring of coffee roasting by resonant laser ionisation time-of-flight mass spectrometry: bridging the gap from industrial batch roasting to flavour formation inside an individual coffee bean *Journal of mass spectrometry : JMS* 48:1253-1265 doi:10.1002/jms.3299

- Hertz-Schunemann R, Streibel T, Ehlert S, Zimmermann R (2013b) Looking into individual coffee beans during the roasting process: direct micro-probe sampling on-line photo-ionisation mass spectrometric analysis of coffee roasting gases *Anal Bioanal Chem* 405:7083-7096 doi:10.1007/s00216-013-7006-y
- Hof F, Schäfer RA, Weiss C, Hauke F, Hirsch A (2014) Novel  $\lambda$ 3-Iodane-Based Functionalization of Synthetic Carbon Allotropes (SCAs)—Common Concepts and Quantification of the Degree of Addition Chemistry – *A European Journal* 20:16644-16651 doi:10.1002/chem.201404662
- Hölzer J et al. (2014) Hyphenation of thermogravimetry and soft single photon ionization–ion trap mass spectrometry (TG–SPI–ITMS) for evolved gas analysis *J Therm Anal Calorim* 116:1471-1479 doi:10.1007/s10973-014-3826-z
- Isaacman G et al. (2012) Improved Resolution of Hydrocarbon Structures and Constitutional Isomers in Complex Mixtures Using Gas Chromatography-Vacuum Ultraviolet-Mass Spectrometry *Analytical Chemistry* 84:2335-2342 doi:10.1021/ac2030464
- Jia L et al. (2015) Fast Pyrolysis in a Microfluidized Bed Reactor: Effect of Biomass Properties and Operating Conditions on Volatiles Composition as Analyzed by Online Single Photoionization Mass Spectrometry *Energy Fuels* 29:7364-7374 doi:10.1021/acs.energyfuels.5b01803
- Kaisersberger E, Post E (1997) Practical aspects for the coupling of gas analytical methods with thermal-analysis instruments *Thermochimica Acta* 295:73-93 doi:10.1016/s0040-6031(97)00099-3
- Kaisersberger E, Post E (1998) Applications for skimmer coupling systems, combining simultaneous thermal analysers with mass spectrometers *Thermochimica Acta* 324:197-201 doi:10.1016/s0040-6031(98)00536-x
- Krist S, Unterweger H, Bandion F, Buchbauer G (2004) Volatile compound analysis of SPME headspace and extract samples from roasted Italian chestnuts (*Castanea sativa* Mill.) using GC-MS *Eur Food Res Technol* 219:470-473 doi:10.1007/s00217-004-0983-5
- Lindinger W, Hirber J, Paretzke H (1993) An ion/molecule-reaction mass spectrometer used for on-line trace gas analysis *International Journal of Mass Spectrometry and Ion Processes* 129:79-88 doi:10.1016/0168-1176(93)87031-m
- Mason ME, Johnson B, Hamming MC (1967) Volatile components of roasted peanuts. Major monocarbonyls and some noncarbonyl components *Journal of Agricultural and Food Chemistry* 15:66-73 doi:10.1021/jf60149a029
- Materazzi S, Risoluti R (2014) Evolved Gas Analysis by Mass Spectrometry *Appl Spectrosc Rev* 49:635-665 doi:10.1080/05704928.2014.887021
- Materazzi S, Vecchio S (2013) Recent Applications of Evolved Gas Analysis by Infrared Spectroscopy (IR-EGA) *Appl Spectrosc Rev* 48:654-689 doi:10.1080/05704928.2013.786722
- Matsui T, Guth H, Grosch W (1998) A comparative study of potent odorants in peanut, hazelnut, and pumpkin seed oils on the basis of aroma extract dilution analysis (AEDA) and gas chromatography olfactometry of headspace samples (GCOH) *Fett-Lipid* 100:51-56
- Mottram D (2007) The Maillard Reaction: Source of Flavour in Thermally Processed Foods. In: Berger R (ed) *Flavours and Fragrances*. Springer Berlin Heidelberg, pp 269-283. doi:10.1007/978-3-540-49339-6\_12
- Neta ER, Sanders T, Drake MA (2010) Understanding Peanut Flavor: A Current Review. In: *Handbook of Fruit and Vegetable Flavors*. John Wiley & Sons, Inc., pp 985-1022. doi:10.1002/9780470622834.ch51
- Raemakers KGH, Bart JCJ (1997) Applications of simultaneous thermogravimetry-mass spectrometry in polymer analysis *Thermochimica Acta* 295:1-58 doi:10.1016/s0040-6031(97)00097-x
- Rüger CP, Miersch T, Schwemer T, Sklorz M, Zimmermann R (2015) Hyphenation of Thermal Analysis to Ultrahigh-Resolution Mass Spectrometry (Fourier Transform Ion Cyclotron Resonance Mass Spectrometry) Using Atmospheric Pressure Chemical Ionization For Studying Composition and Thermal Degradation of Complex Materials *Analytical Chemistry* doi:10.1021/acs.analchem.5b00785

- Saraji-Bozorgzad MR et al. (2010) Highly Resolved Online Organic-Chemical Speciation of Evolved Gases from Thermal Analysis Devices by Cryogenically Modulated Fast Gas Chromatography Coupled to Single Photon Ionization Mass Spectrometry *Analytical Chemistry* 82:9644-9653 doi:10.1021/ac100745h
- Saraji-Bozorgzad MR, Streibel T, Kaisersberger E, Denner T, Zimmermann R (2011) Detection of organic products of polymer pyrolysis by thermogravimetry-supersonic jet-skimmer time-of-flight mass spectrometry (TG-Skimmer-SPI-TOFMS) using an electron beam pumped rare gas excimer VUV-light source (EBEL) for soft photo ionisation *J Therm Anal Calorim* 105:691-697 doi:10.1007/s10973-011-1383-2
- Schirack AV, Drake MA, Sanders TH, Sandeep KP (2006) Characterization of Aroma-Active Compounds in Microwave Blanched Peanuts *Journal of Food Science* 71:C513-C520 doi:10.1111/j.1750-3841.2006.00173.x
- Schmid P, Stöhr F, Arndt M, Tüxen J, Mayor M (2013) Single-Photon Ionization of Organic Molecules Beyond 10 kDa *J Am Soc Mass Spectrom* 24:602-608 doi:10.1007/s13361-012-0551-3
- Smith AL, Barringer SA (2014) Color and Volatile Analysis of Peanuts Roasted Using Oven and Microwave Technologies *Journal of Food Science* 79:C1895-C1906 doi:10.1111/1750-3841.12588
- Streibel T, Mitschke S, Adam T, Weh J, Zimmermann R (2007) Thermal desorption/pyrolysis coupled with photo ionisation time-of-flight mass spectrometry for the analysis and discrimination of pure tobacco samples *Journal of Analytical and Applied Pyrolysis* 79:24-32 doi:10.1016/j.jaap.2006.12.017
- Su G, Zheng L, Cui C, Yang B, Ren J, Zhao M (2011) Characterization of antioxidant activity and volatile compounds of Maillard reaction products derived from different peptide fractions of peanut hydrolysate *Food Research International* 44:3250-3258 doi:10.1016/j.foodres.2011.09.009
- Várhegyi G, Czégény Z, Jakab E, McAdam K, Liu C (2009) Tobacco pyrolysis. Kinetic evaluation of thermogravimetric–mass spectrometric experiments *Journal of Analytical and Applied Pyrolysis* 86:310-322 doi:10.1016/j.jaap.2009.08.008
- Walradt JP, Pittet AO, Kinlin TE, Muralidhara R, Sanderson A (1971) Volatile components of roasted peanuts *Journal of Agricultural and Food Chemistry* 19:972-979 doi:10.1021/jf60177a017
- Wilbrandt S, Stenzel O, Heiße H, Kaiser N (2012) Dielektrisch verstärkte Aluminiumspiegel für VUV-Anwendungen *Vakuum in Forschung und Praxis* 24:41-46 doi:10.1002/vipr.201290069
- Wohlfahrt S et al. (2013) Rapid comprehensive characterization of crude oils by thermogravimetry coupled to fast modulated gas chromatography-single photon ionization time-of-flight mass spectrometry *Anal Bioanal Chem* 405:7107-7116 doi:10.1007/s00216-013-7029-4
- Wu Q et al. (2010) A combined single photon ionization and photoelectron ionization source for orthogonal acceleration time-of-flight mass spectrometer *International Journal of Mass Spectrometry* 295:60-64 doi:10.1016/j.ijms.2010.06.034
- Yang Z, Zhang T, Pan Y, Hong X, Tang Z, Qi F (2009) Electrospray/VUV Single-Photon Ionization Mass Spectrometry for the Analysis of Organic Compounds *J Am Soc Mass Spectrom* 20:430-434 doi:10.1016/j.jasms.2008.10.026
- Yeretzian C, Jordan A, Lindinger W (2003) Analysing the headspace of coffee by proton-transfer-reaction mass-spectrometry *International Journal of Mass Spectrometry* 223–224:115-139 doi:10.1016/S1387-3806(02)00785-6
- Zimmermann R, Hertz-Schünemann R, Ehlert S, Liu C, McAdam K, Baker R, Streibel T (2015) Highly Time-Resolved Imaging of Combustion and Pyrolysis Product Concentrations in Solid Fuel Combustion: NO Formation in a Burning Cigarette *Analytical Chemistry* 87:1711-1717 doi:10.1021/ac503512a



Supporting Information for article

## **Online analysis of volatile compounds formation during gentle roasting of various nut seeds using thermogravimetry coupled to fast cycling gas chromatography-mass spectrometry**

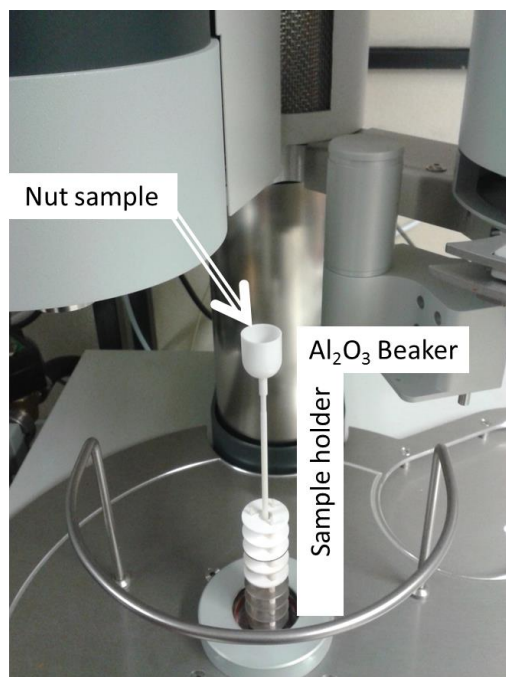
Michael Fischer<sup>1,2</sup>, Sebastian Wohlfahrt<sup>1,2</sup>, Janos Varga<sup>2,3</sup>, Georg Matuschek<sup>4</sup>, Mohammad R. Saraji-Bozorgzad<sup>5</sup>, Thomas Denner<sup>6</sup>, Andreas Walte<sup>7</sup>, Ralf Zimmermann<sup>\*,1,2</sup>

- [1] Joint Mass Spectrometry Centre, Institute of Chemistry, Chair of Analytical Chemistry, University of Rostock, 18057 Rostock, Germany
- [2] Joint Mass Spectrometry Centre, Cooperation Group “Comprehensive Molecular Analytics”, Helmholtz Zentrum München, 85764 Neuherberg, Germany
- [3] University of Augsburg, Chair of Resource Strategy, 86159 Augsburg, Germany
- [4] Research Unit Medical Radiation Physics and Diagnostics, Helmholtz Zentrum München, 85764 Neuherberg, Germany
- [5] Photonion GmbH, 85764 Neuherberg, Germany
- [6] Netzsch-Geraetebau GmbH, 95100 Selb, Germany
- [7] Airsense Analytics GmbH, 19061 Schwerin, Germany

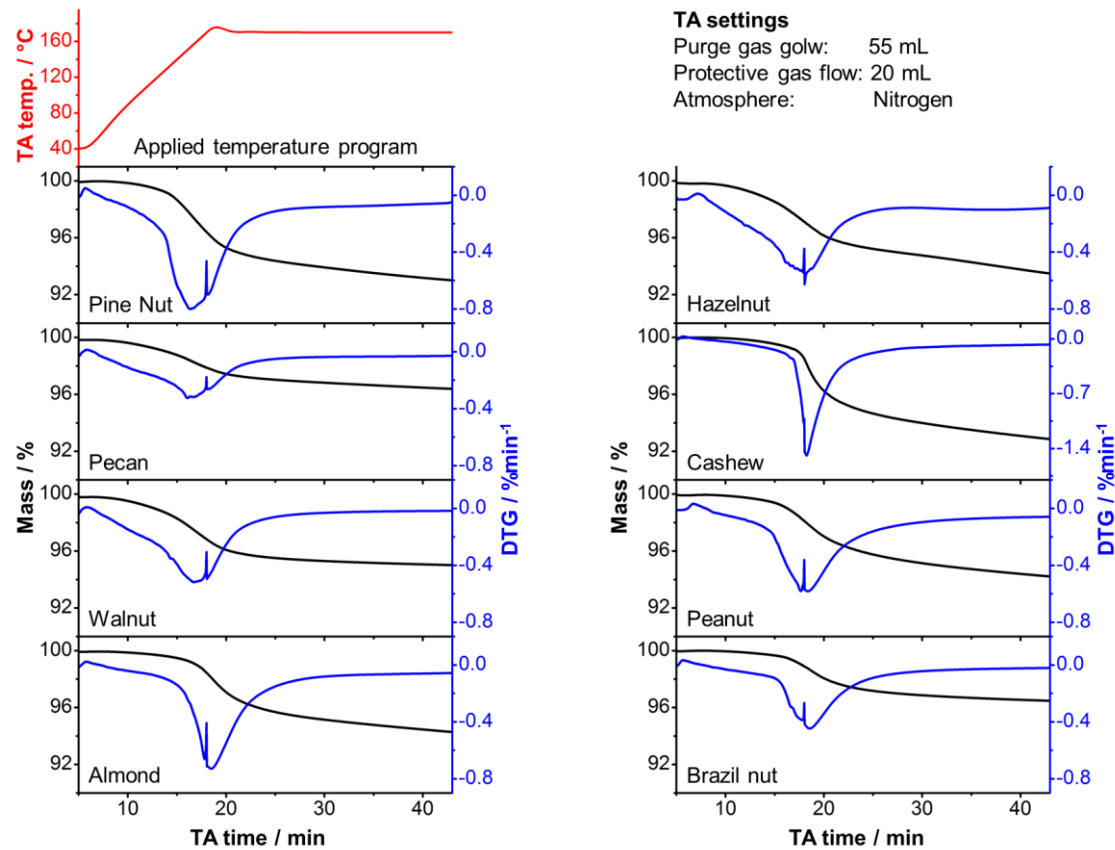
\* Corresponding author: ralf.zimmermann@helmholtz-muenchen.de, or ralf.zimmermann@uni-rostock.de. Tel.: +49 (0) 89 3187 4544. Fax: +49 (0) 89 3187 3371. Supply all supplementary material in standard file formats.

## Table of contents

Figure S-1	TA sample carrier “beaker”.
Figure S-2	TA-data for almond, brazil nut, cashew, peanut, hazelnut, pecan, pine nut and walnut.
Figure S-3	DTG-data for four peanuts to show repeatability.
Figure S-4	Comparison of the ratios from m/z 94 and m/z 108 in three peanut roasting experiments.
Table S-1	EI and SPI mass spectra of the assigned compounds listed in Table 1 and their related EI mass spectra from NIST

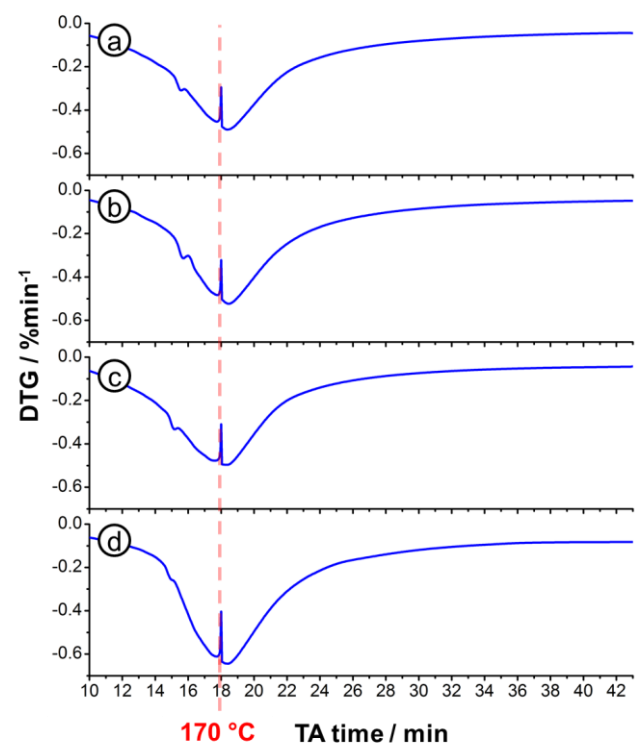


**Figure S-1.** The nut sample is directly placed in the sample carrier (Al<sub>2</sub>O<sub>3</sub> Beaker) of the STA 449 F3 Jupiter. In this configuration only thermogravimetric data generation is possible.

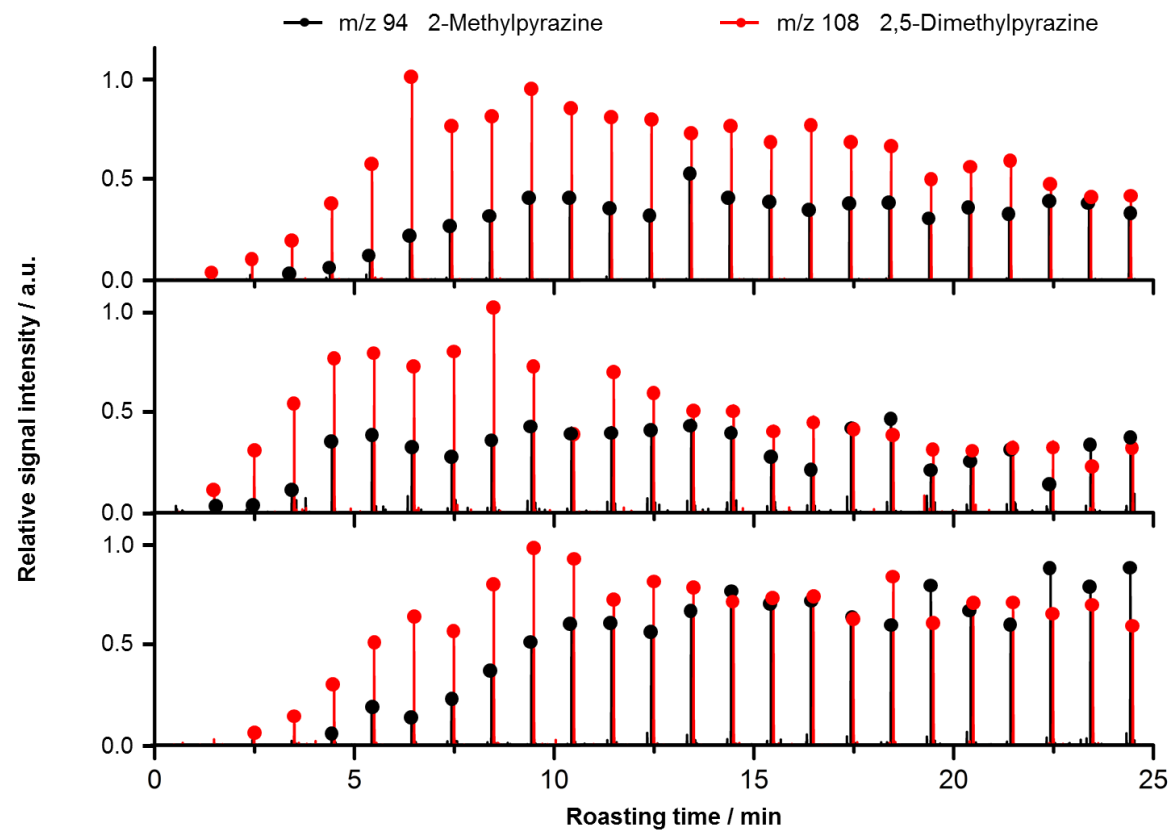


**Figure S-2.** TA-Data of almond, brazil nut, cashew, peanut, hazelnut, pecan, pine nut and walnut, recorded during the roasting process. The mass loss and its first derivative show differences at the beginning while the various nuts are heated up and continue for a little while. These signals are dedicated to the loss of water. In the ongoing roasting process,

there are no significant differences. The study shows that the TA signals can't provide supporting information about the composition of the roast gases. The arising in the DTG-signal of every measurement is merely the effect when the temperature of 170°C is reached (depending on the nuts' properties) and is therefore classified to be artificial.

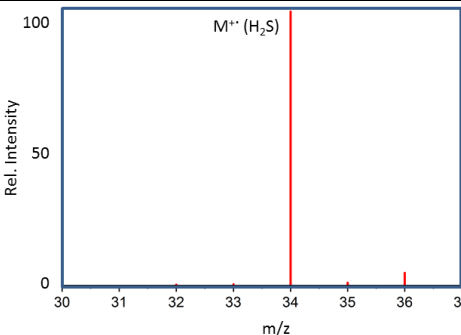
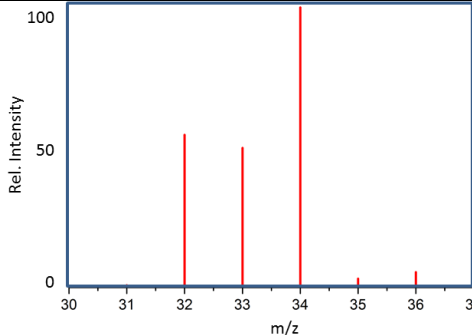
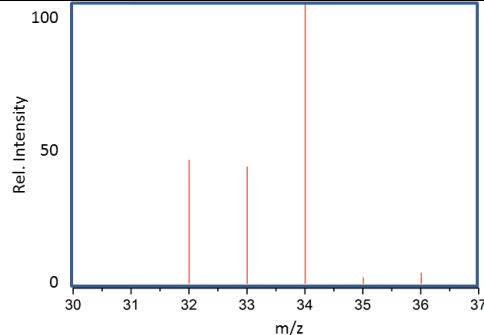


**Figure S-3.** DTG-data of four peanut samples (a-d) are evaluated and show repeatability and thereby the similarity of one nut species. The artificial signal, as mentioned in Figure S-2 appears when the roasting temperature of 170 °C, after 18 min in the TA is reached.

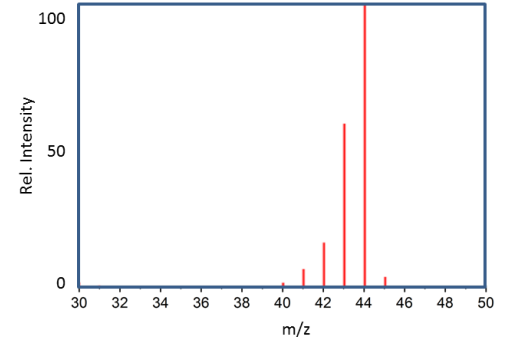
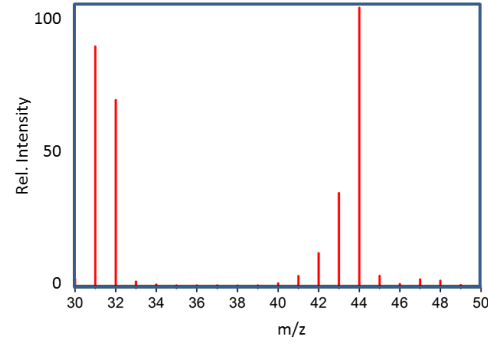
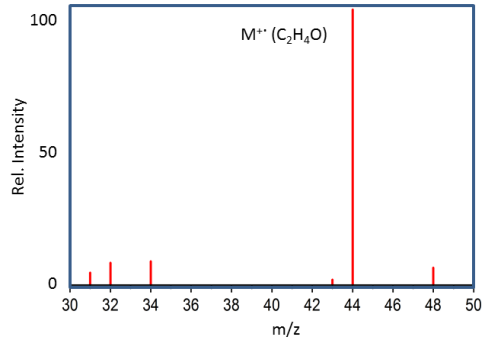


**Figure S-4.** The SICs of m/z 94 (2-methylpyrazine) and m/z 108 (2,5-dimethylpyrazine) in three peanut samples during roasting at 170 °. Signal intensities vary between the single nut samples, but the trend of the ratios is comparable. 2,5-dimethylpyrazine is dominating in the beginning, In the end m/z 94 and m/z 108 contribute equally.

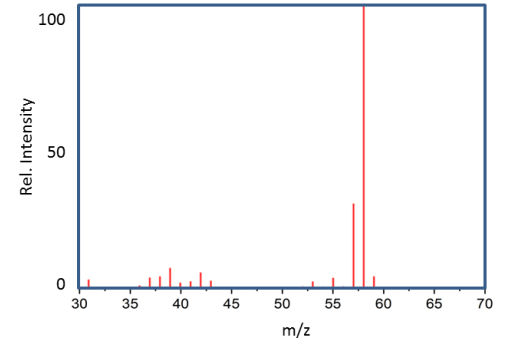
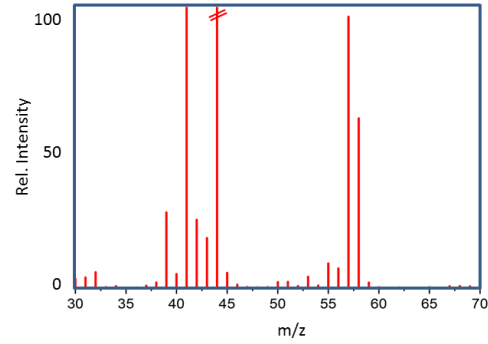
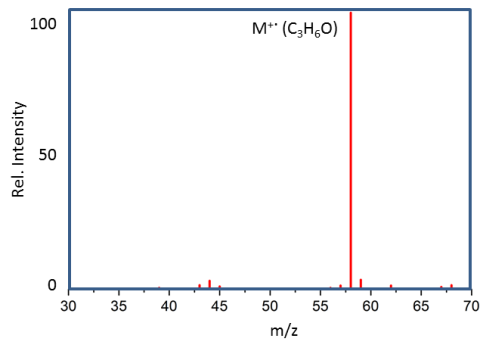
**Table S-1.** List of compounds detected in the roast gases and assigned by comparison of the EI mass spectrum to the NIST EI mass spectrum and compared to the SPI mass spectrum with the molecular ion information. Additionally, the information of SPI enables to tackle co-eluting compounds. Please note, in the EI mass spectra  $m/z$  44 is almost permanently present (not efficiently modulated  $\text{CO}_2$ ) but was not considered during evaluation.  $M/z < 30$  has been eliminated by the applied mass filter. Thus, mass spectra start with  $m/z$  30 and the range of the NIST mass spectrum has been adapted.

Nr.	$m/z$	CAS Registry Number, Compound	SPI MASS SPECTRUM	EI MASS SPECTRUM	NIST EI MASS SPECTRUM
1	34	7783-06-4, Hydrogen sulfide			

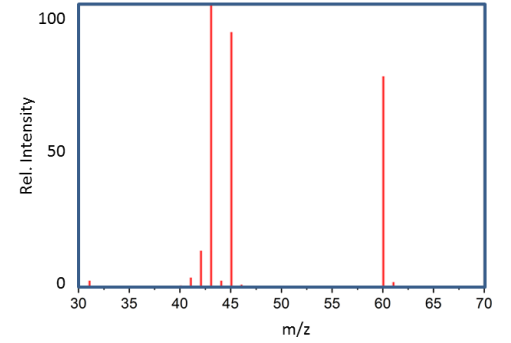
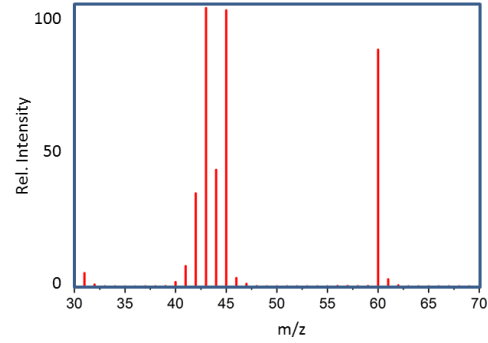
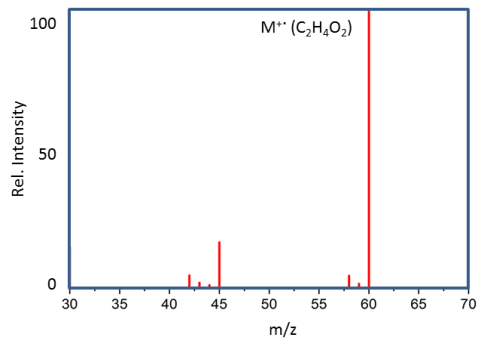
2\* 44 75-07-0,  
Acetaldehyd



3\* 58 123-38-6,  
(123-38-6),  
Propanal  
(Acetone)

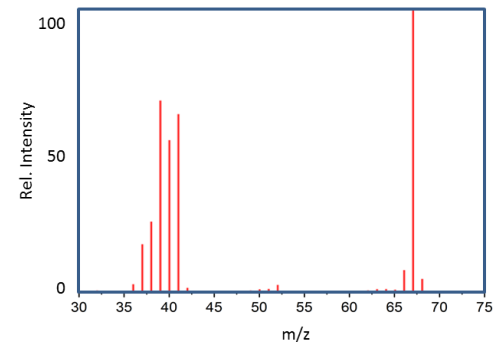
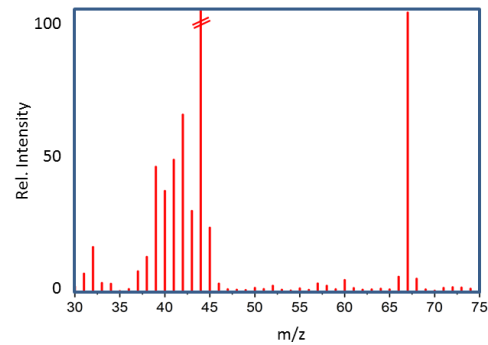
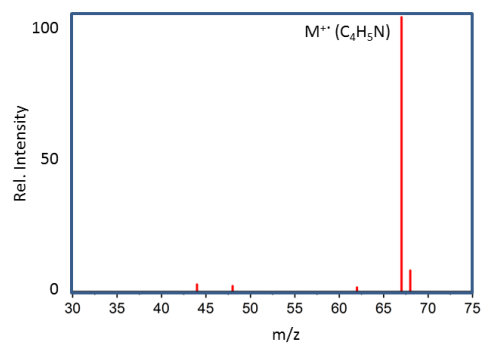


4 60 64-19-7,  
Acetic acid

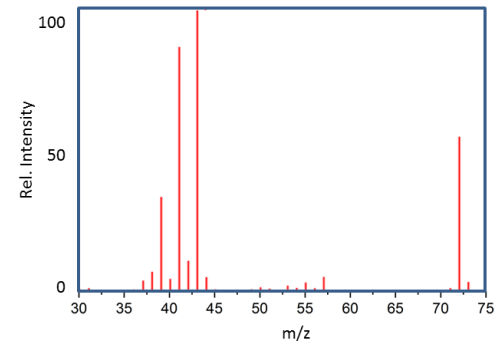
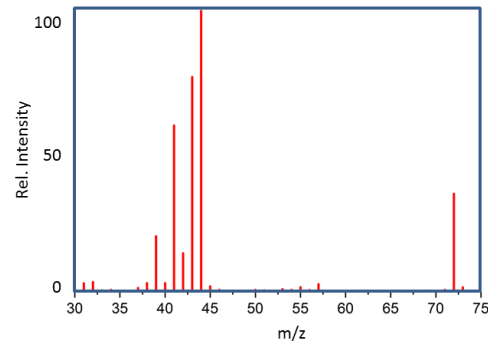
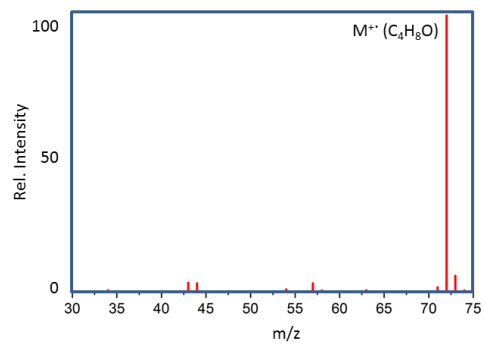




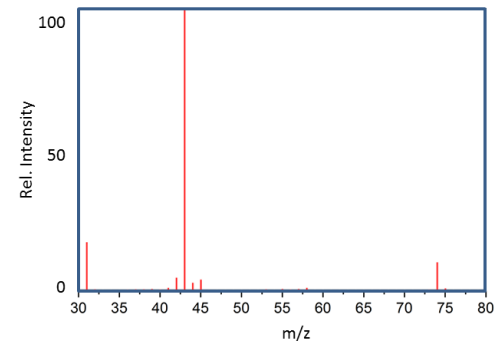
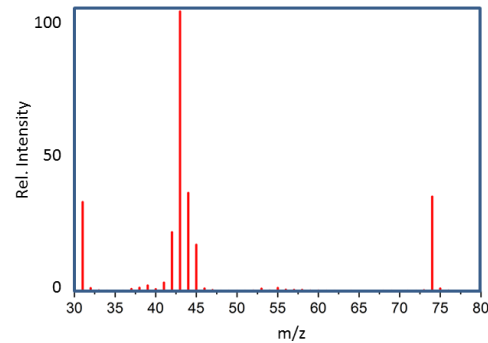
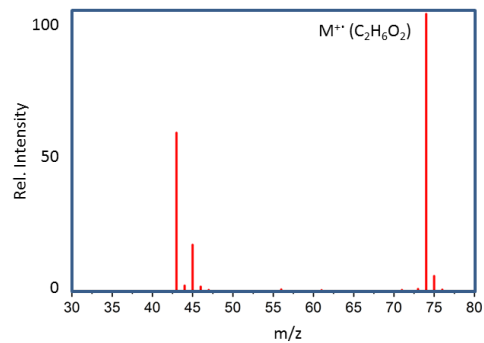
5 67 109-97-7,  
Pyrrole



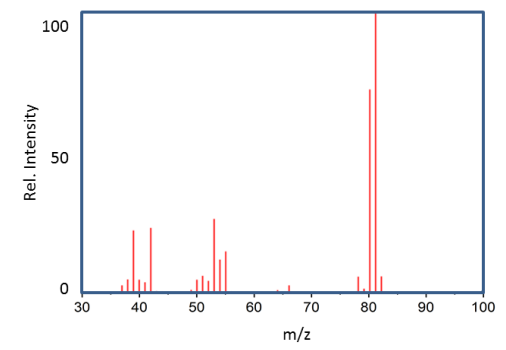
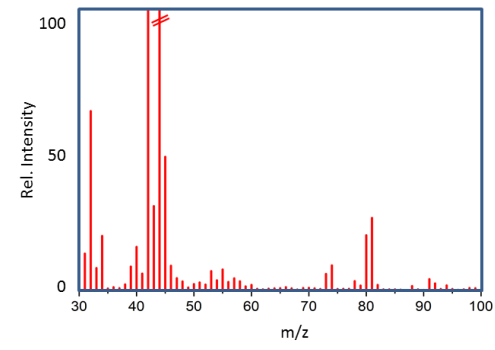
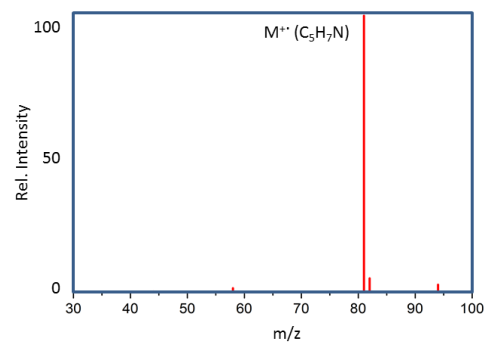
6 72 78-84-2,  
2-Methylprop  
anal



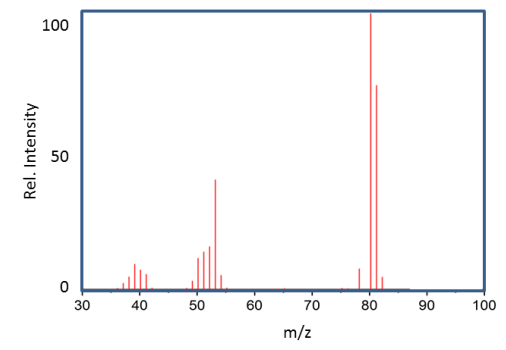
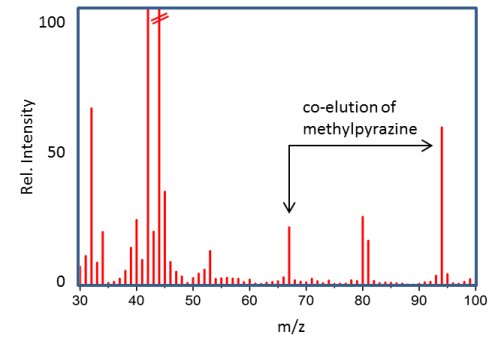
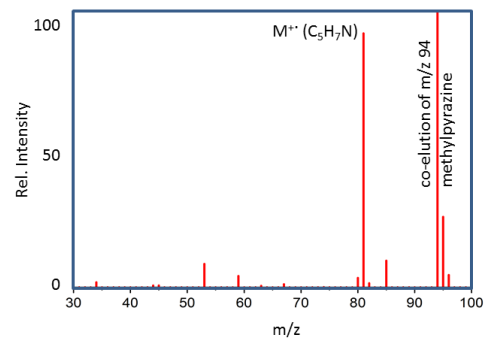
7 74 116-09-6,  
1-Hydroxy-  
2-propanone



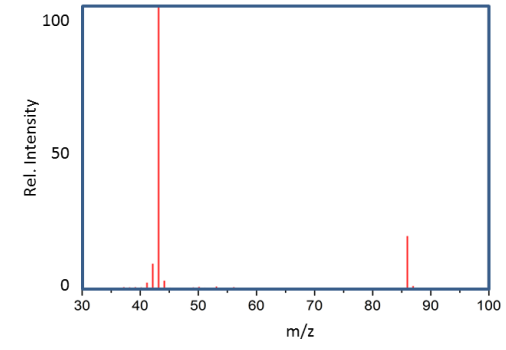
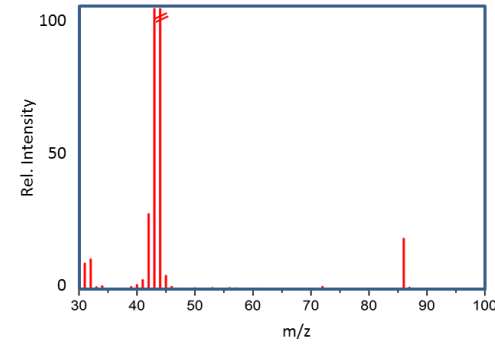
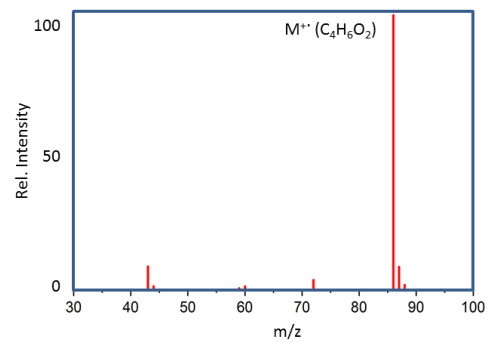
8 81 96-54-8,  
1-Methyl-  
1H-pyrrole



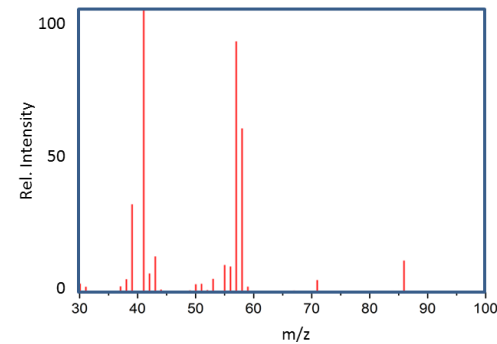
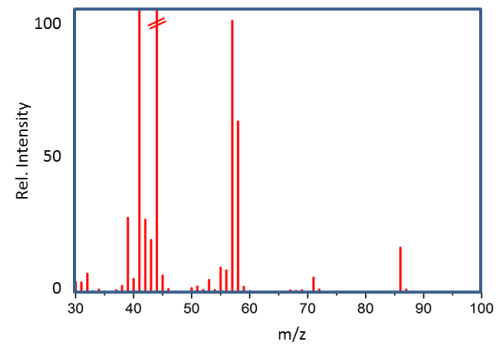
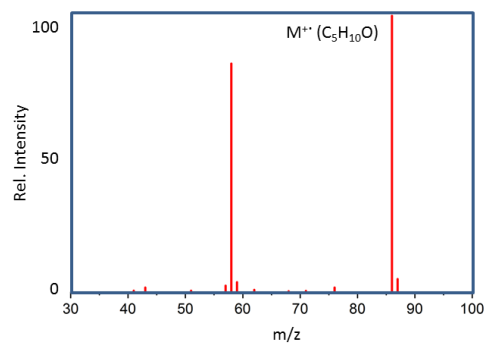
9 81 616-43-3,  
3-Methyl-  
1H-pyrrole



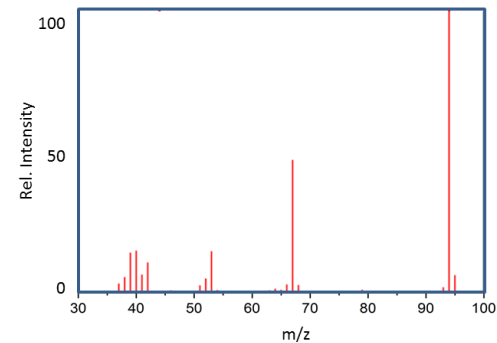
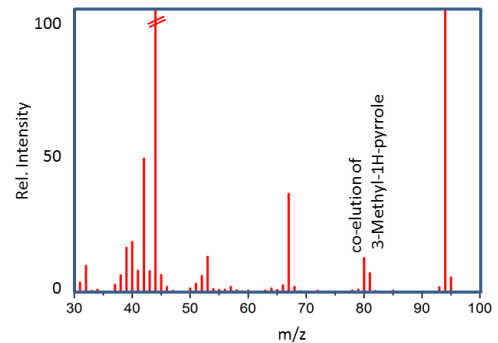
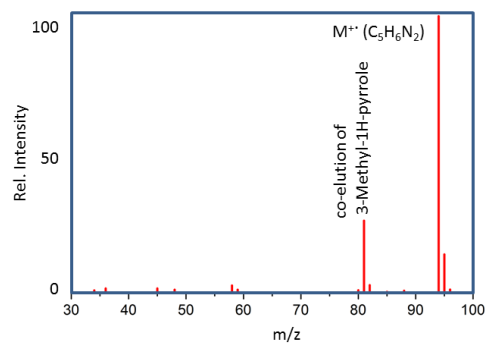
10 86 431-03-8,  
2,3-  
Butanedione



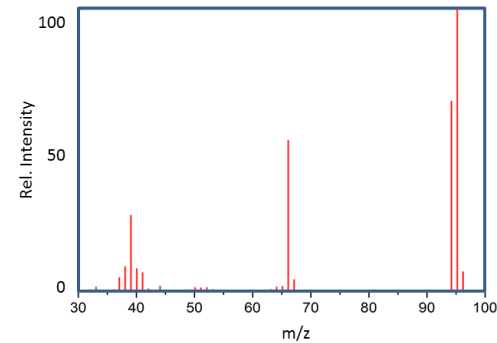
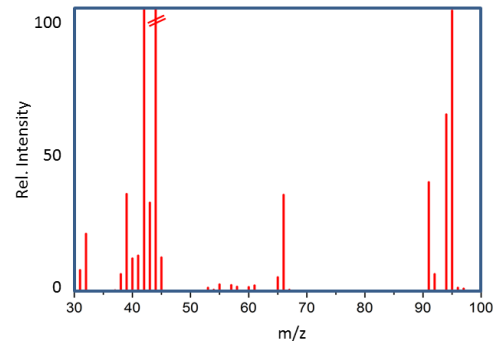
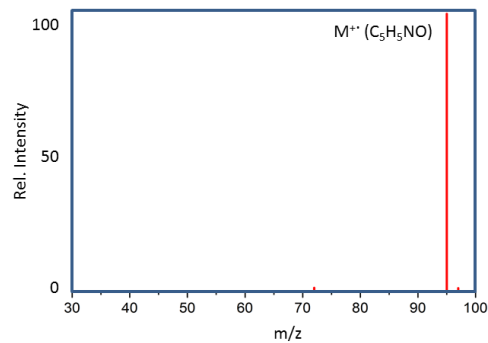
11 86 96-17-3,  
2-  
Methylbuta  
nal



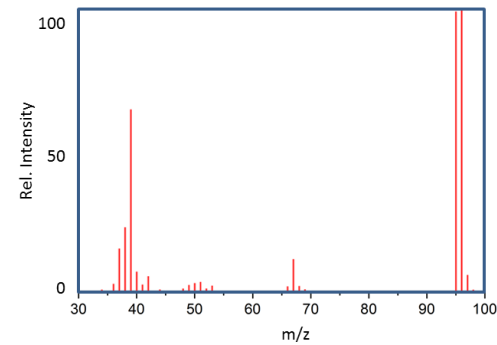
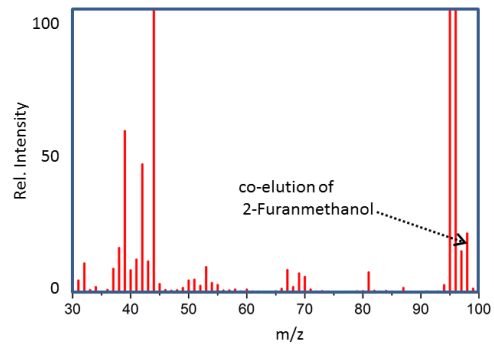
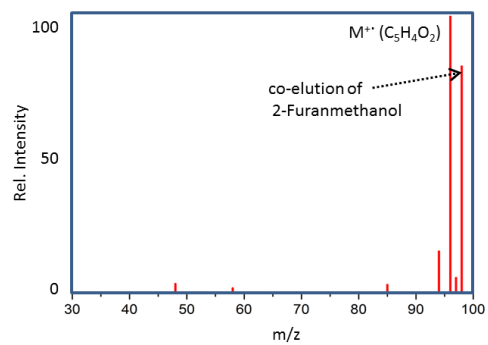
12 94 109-08-0,  
Methylpyra  
zine



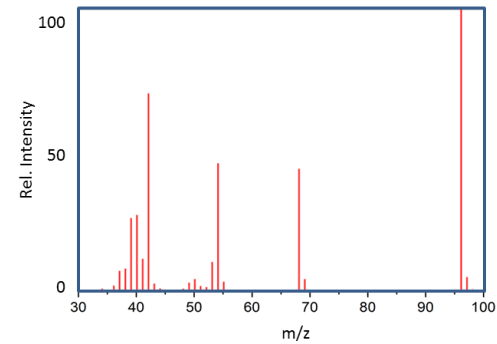
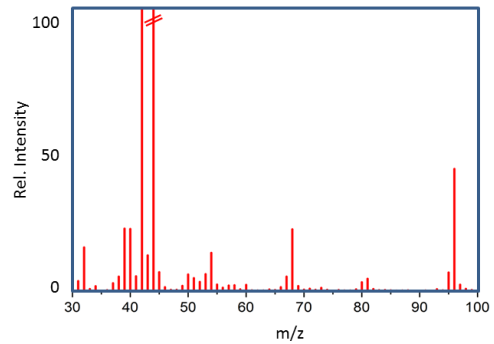
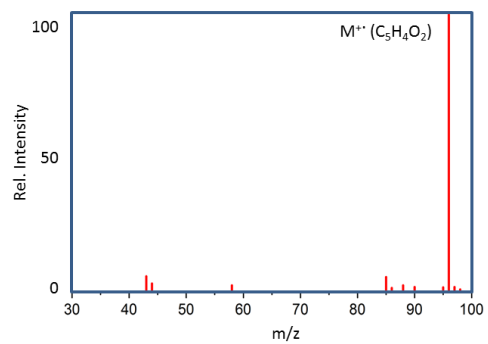
13 95 1003-29-8,  
2-  
Carboxalde  
hyde-1H-  
pyrrole



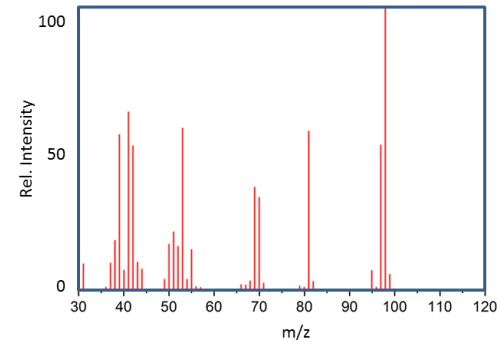
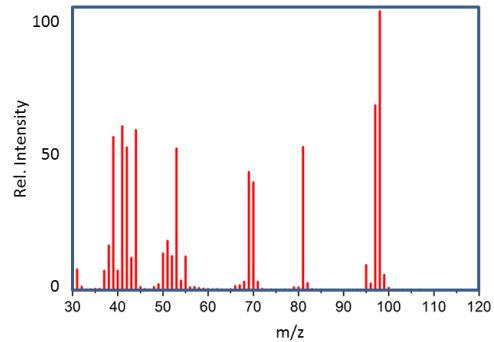
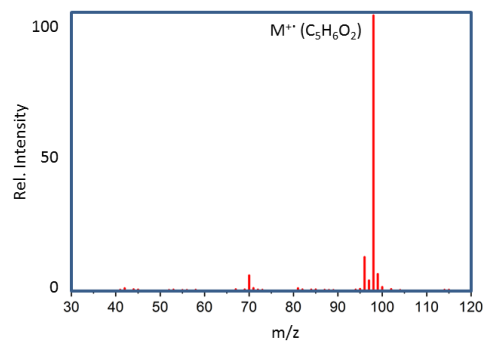
14 96 98-01-1,  
Furfural



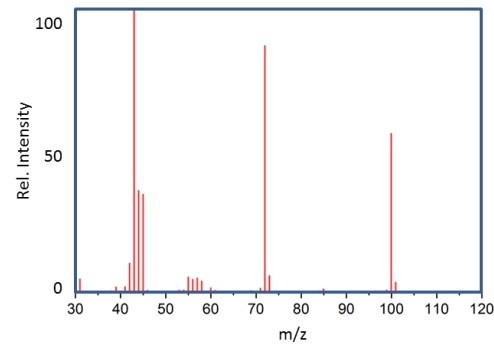
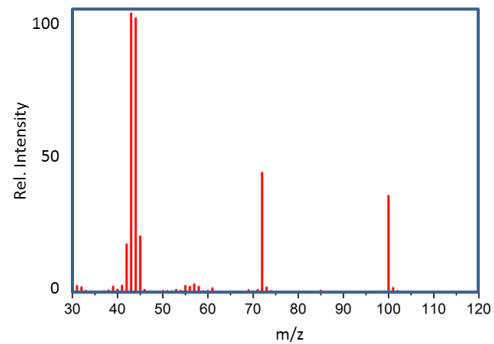
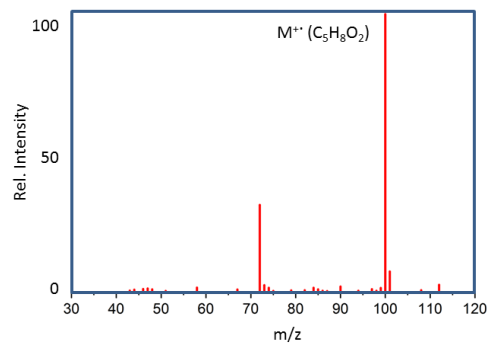
15 96 930-60-9,  
4-  
Cyclopenten  
e-1,3-dione



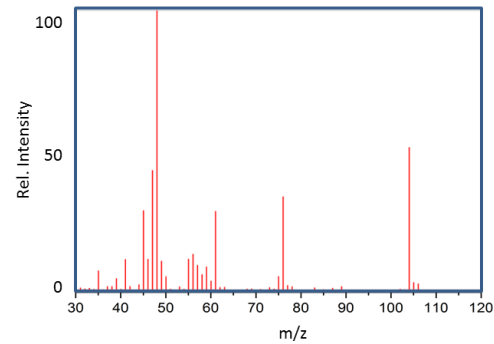
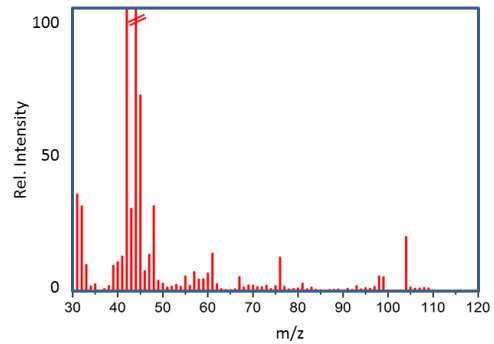
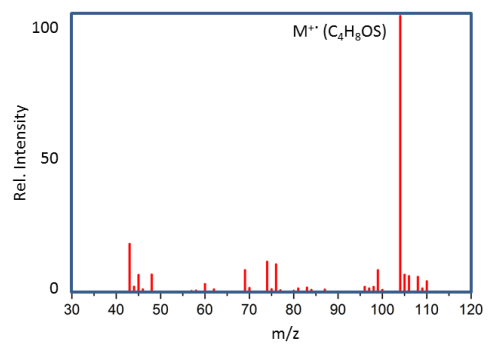
16 98 98-00-0,  
2-  
Furanmetha  
nol



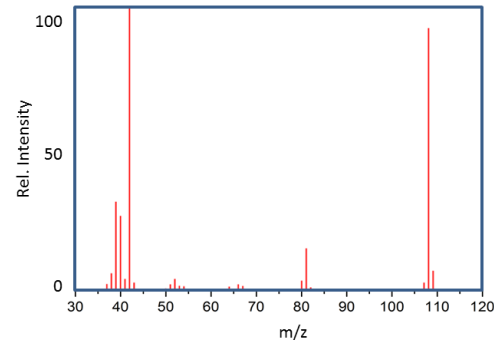
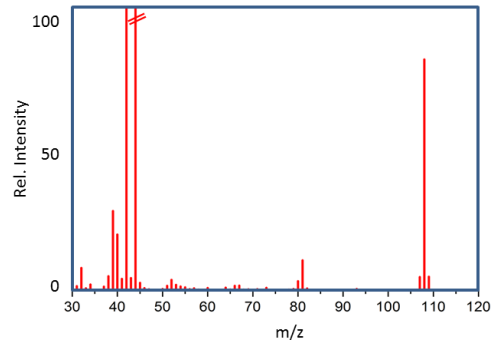
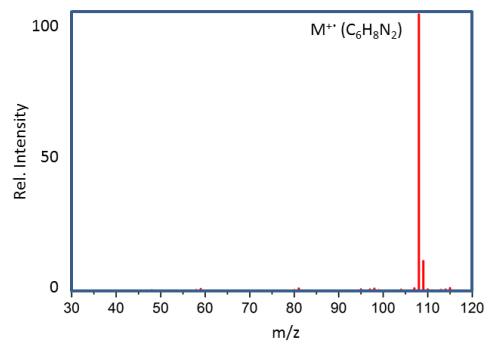
17 100 3188-00-9,  
Dihydro-2-  
methyl-  
3(2H)-  
furanone



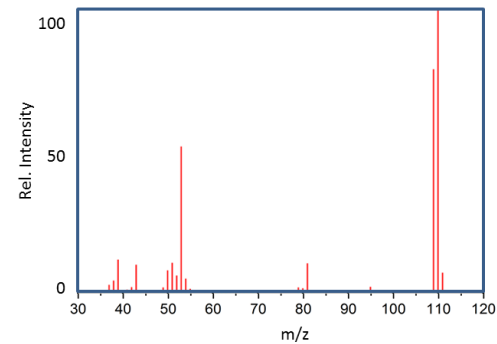
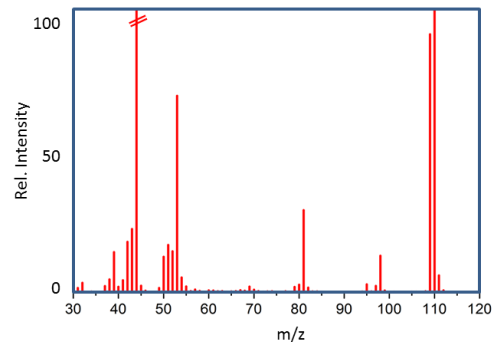
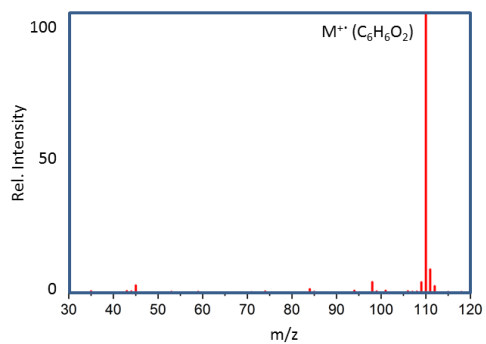
18 104 3268-49-3,  
Methional



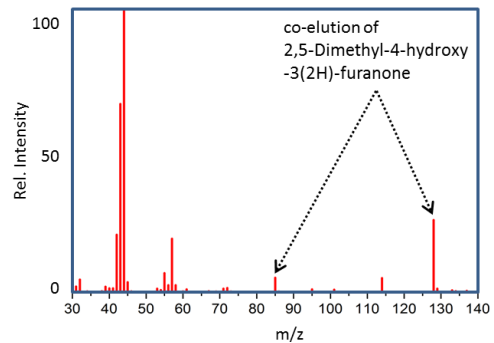
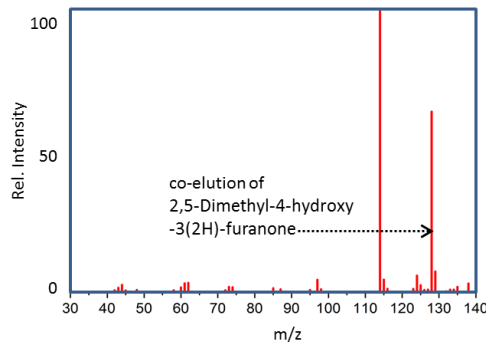
19 108 123-32-0,  
2,5-  
Dimethylpy  
razine



20 110 620-02-0,  
5-Methyl-2-  
furancarbox  
aldehyde

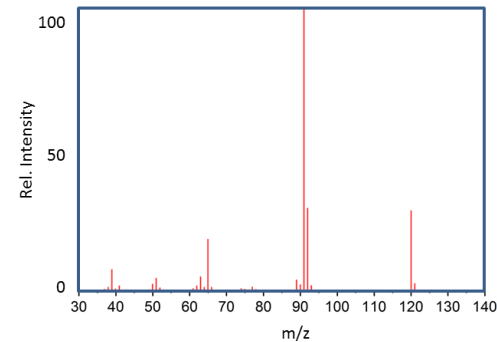
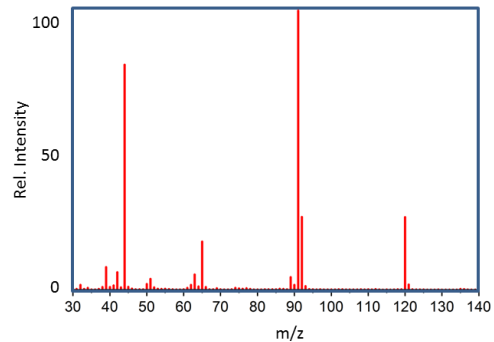
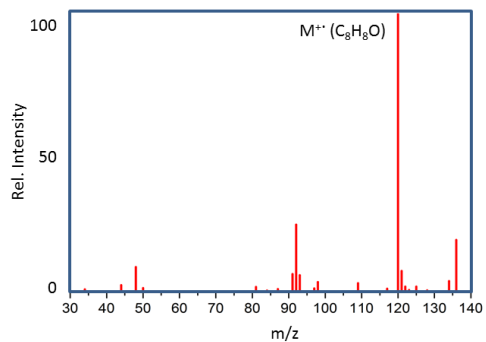


21\* 114 98-02-2,  
110-43-0,  
111-71-7,  
2-  
Furfurylthio  
l, 2-  
heptanone,  
heptanal

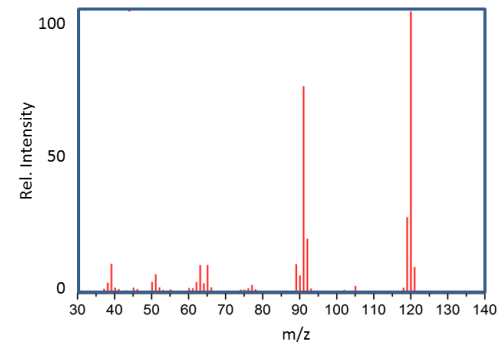
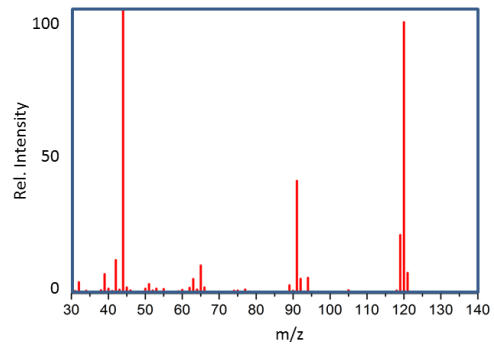
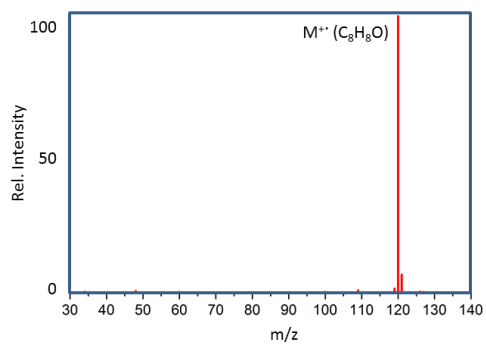


Tentative assignments according to literature:  
Co-eluting with 2,5-Dimethyl-4-hydroxy-  
3(2H)-furanone.

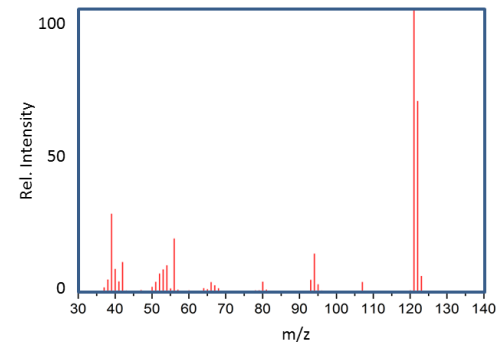
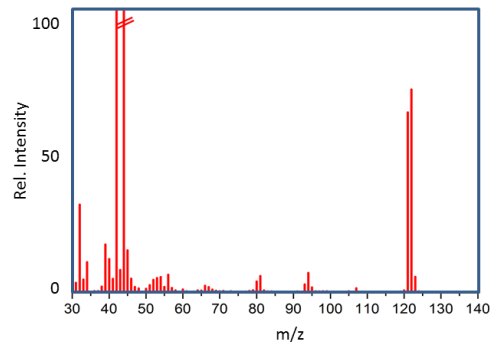
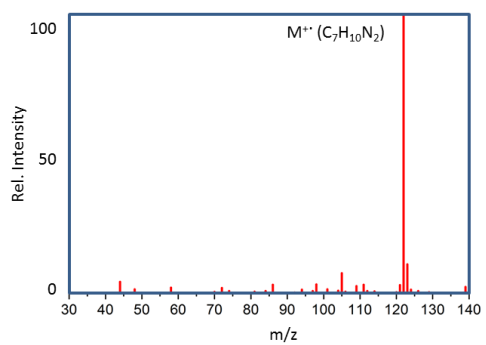
22 120 122-78-1,  
Benzeneacet  
aldehyde



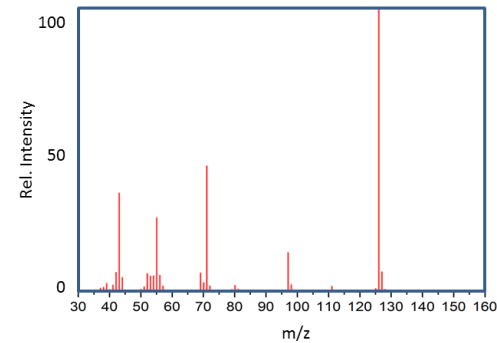
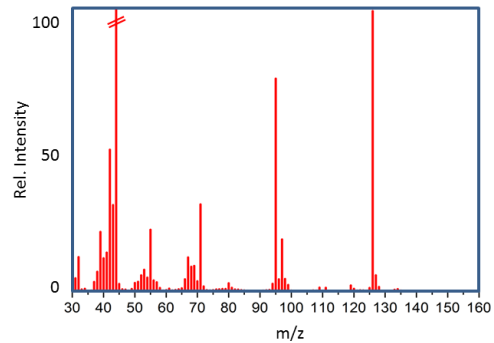
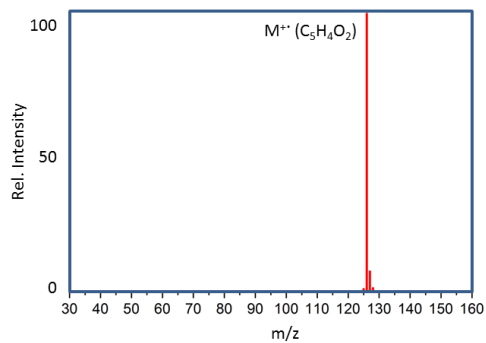
23 120 496-16-2,  
2,3-  
Dihydroben  
zofuran



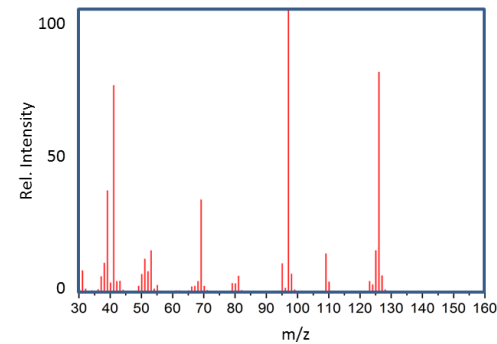
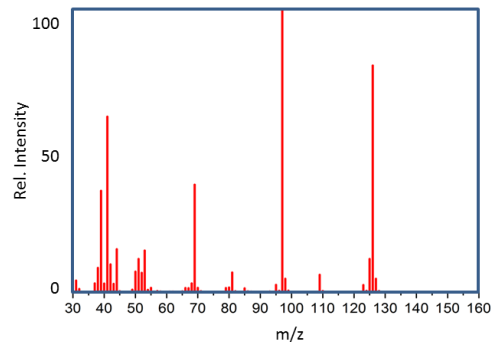
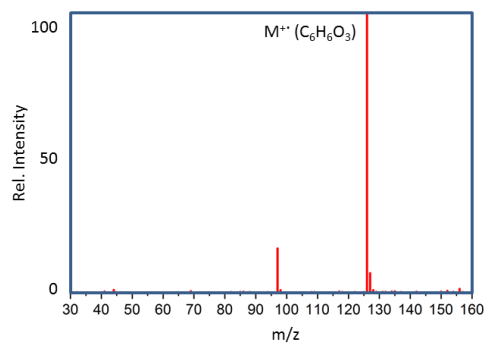
24 122 13360-64-0,  
2-Ethyl-5-  
methylpyraz  
ine



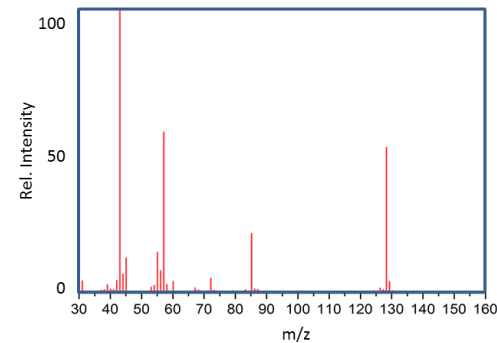
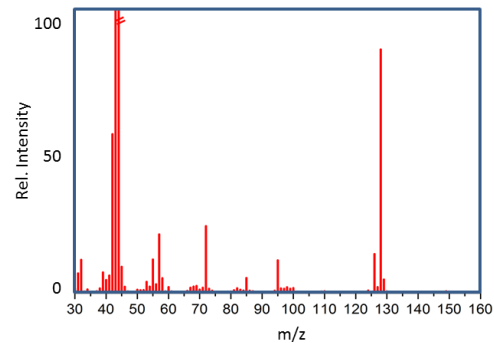
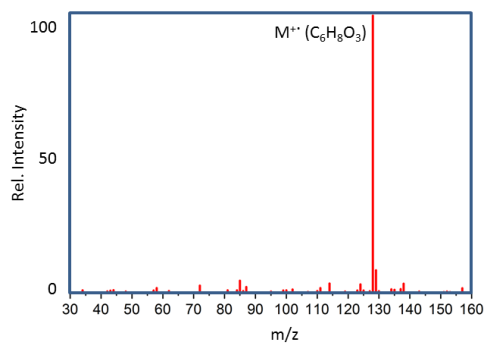
25 126 118-71-8,  
4H-Pyran-4-  
one



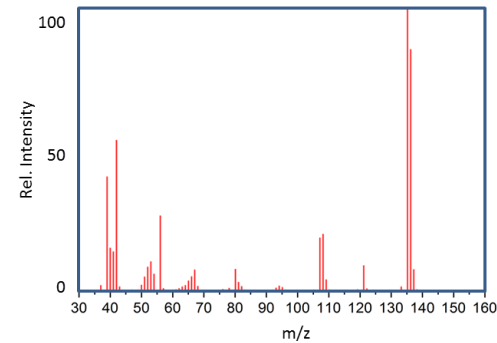
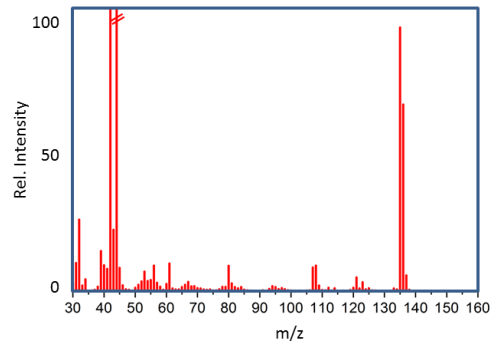
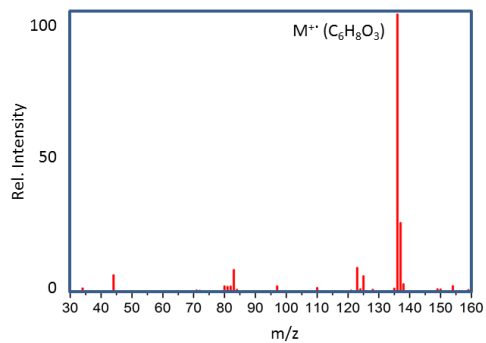
26 126 67-47-0,  
5-  
Hydroxymet  
hylfurfural



27 128 3658-77-3,  
2,5-  
Dimethyl-4-  
hydroxy-  
3(2H)-  
furanone

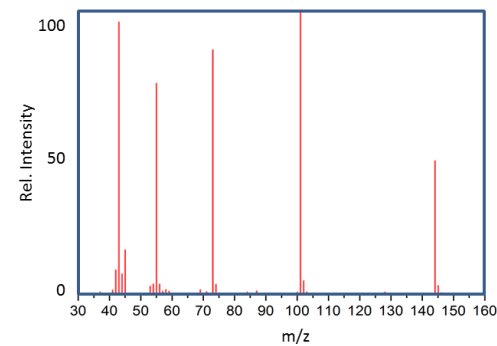
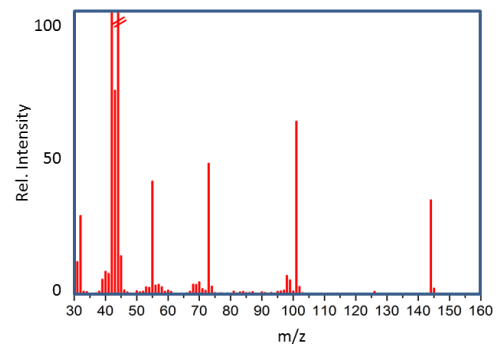
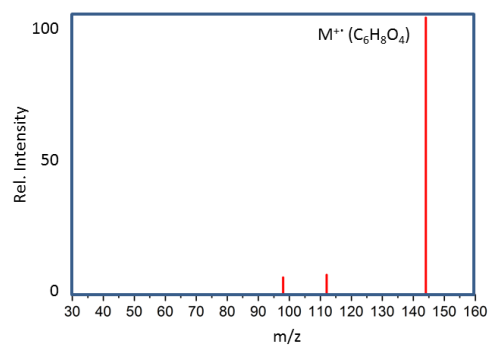


28 136 13360-65-1,  
3-Ethyl-2,5-  
dimethylpyr  
azine

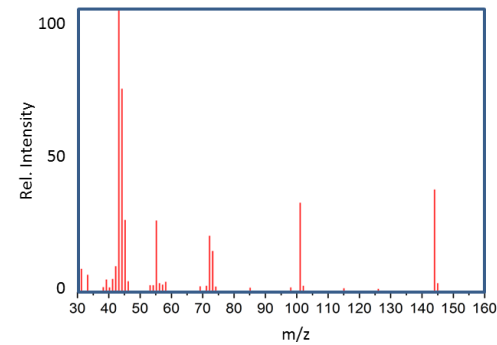
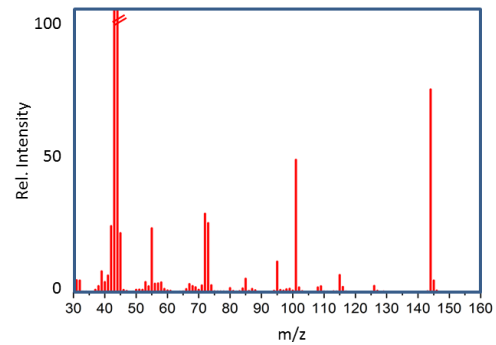
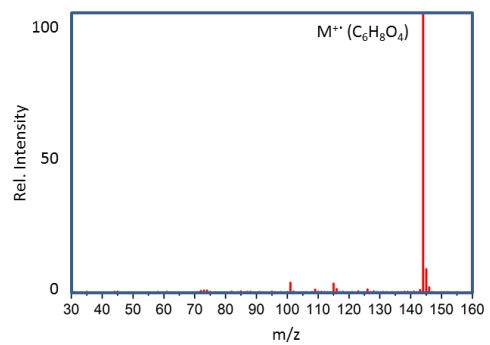




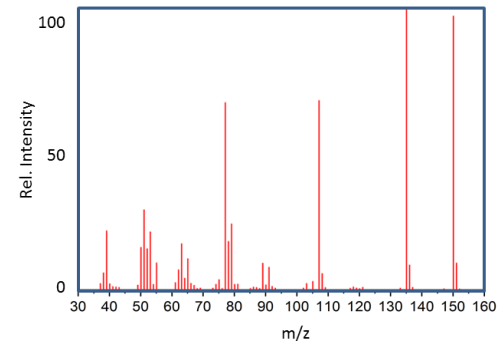
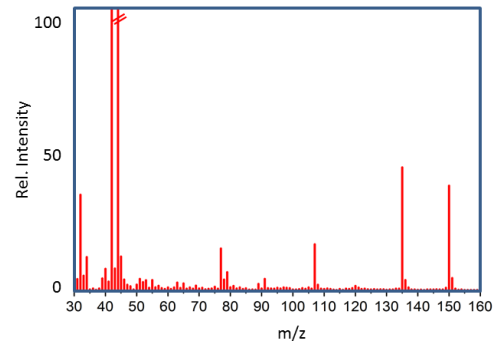
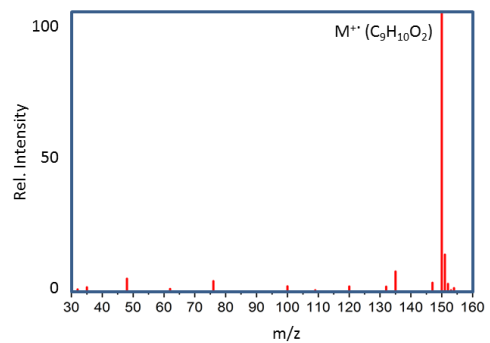
29 144 10230-62-3,  
2,4-  
Dihydroxy-  
2,5-  
dimethyl-  
3(2H)-  
furan-3-one



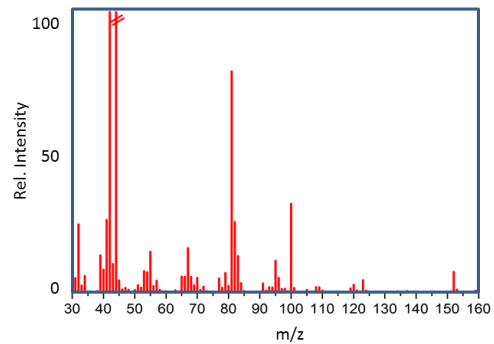
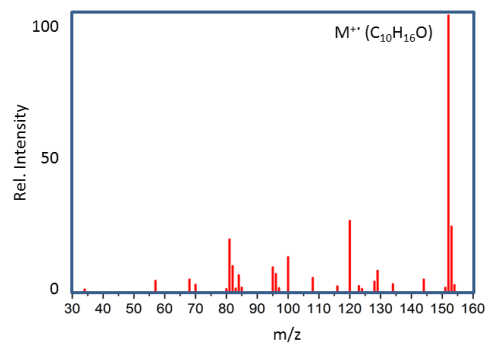
30 144 28564-83-2,  
2,3-  
Dihydro-  
3,5-  
dihydroxy-  
6-methyl-  
4H-pyran-4-  
one



31 150 7786-61-0,  
2-Methoxy-  
4-  
vinylphenol

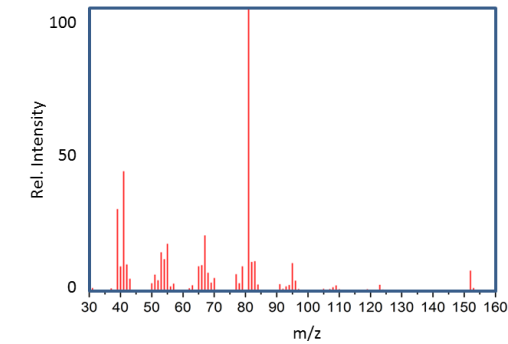
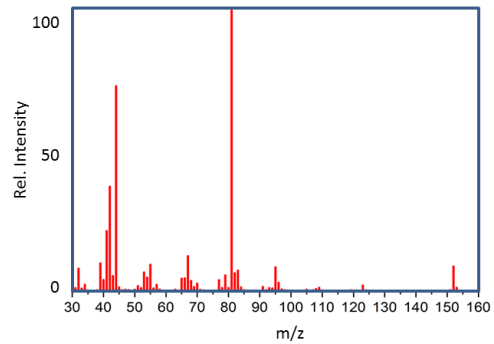
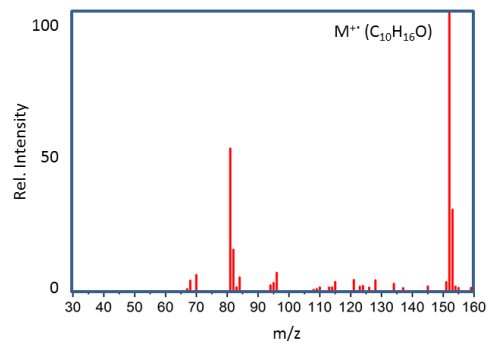


32 152 25152-83-4,  
(E,Z)-2,4-  
Decadienal



Not available at NIST,  
Assigned according to reported RT differences  
from E,E to E,Z (NIST)

33 152 25152-84-5,  
(E,E)-2,4-  
Decadienal



\* No distinct assignment according to the fragment patten possible. Suggestion of possible assignment was done according to literature.